Carderock Division
Naval Surface Warfare Center
9500 MacArthur Blvd.
West Bethesda, MD 20817-5700

NSWCCD-SIG-C98/149-7030 August 1998
Signatures Directorate
Signature Measurement Technology and Systems Development Department

Multiple-Sprung Masses for Wideband Noise Control

by

G. Maidanik
K. Becker

NSWCCD-SIG-C98/149-7320 Multiple Sprung Masses for Wideband Noise Control

SECURITY CLASSIFICATION OF THIS PAGE

REPORT DOCUMENTATION PAGE

Form Approved OMB No. 0704-0188

1a. REPORT SECURITY CLASSIFICATION Unclassified	1b. RESTRICTIVE MARKINGS None
2a. SECURITY CLASSIFICATION AUTHORITY	3. DISTRIBUTION / AVAILABILITY OF REPORT Approved for public release.
2b. DECLASSIFICATION/DOWNGRADING SCHEDULE	Distribution is unlimited
4. PERFORMING ORGANIZATION REPORT NUMBER(S) NSWCCD-SIG-98-/149-7030	5. MONITORING ORGANIZATION REPORT NUMBER(S)
6a. NAME OF PERFORMING ORGANIZATION NSWC, Carderock Division 6b. OFFICE SYMBOL *(If applicable)* Code 7030	7a. NAME OF MONITORING ORGANIZATION
6c. ADDRESS *(City, State, and ZIP Code)* 9500 MacArthur Blvd West Bethesda, MD 20817-5700	7b. ADDRESS *(City, State, and ZIP Code)*
8a. NAME OF FUNDING/SPONSORING ORGANIZATION 8b. OFFICE SYMBOL *(If applicable)*	9. PROCUREMENT INSTRUMENT IDENTIFICATION NUMBER
8c. ADDRESS *(City, State, and ZIP Code)*	10. SOURCE OF FUNDING NUMBERS PROGRAM ELEMENT NO. / PROJECT NO. / TASK NO. / WORK UNIT ACCESSION NO.

11. TITLE *(Include Security Classification)*
Multiple-Sprung Masses for Wideband Noise Control

12. PERSONAL AUTHOR(S)
G. Maidanik and K.J. Becker

13a. TYPE OF REPORT	13b. TIME COVERED	14. DATE OF REPORT *(Year, Month, Day)*	15. PAGE COUNT
Research & Development	FROM 980101 TO 980831	1998 August 31	66

16. SUPPLEMENTARY NOTATION

17. COSATI CODES		
FIELD	GROUP	SUB-GROUP

18. SUBJECT TERMS *(Continue on reverse if necessary and identify by block number)*
Structural Fuzzy Sprung Masses Vibration Control Devices
Joint Impedance Wideband Noise Control

19. ABSTRACT *(Continue on reverse if necessary and identify by block number)*

The design of a wide frequency band neutralizer, vibration absorber and/or structural fuzzy, in the form of multiple sprung masses, is extensively reported in the open literature. The action of the device is reported in terms of the joint point impedance of the sprung masses. This joint impedance is merely the sum over the impedances of the individual sprung masses at the common point to which the device is to be attached to a master structure. The normalized frequency bandwidth of a device composed of a single sprung mass is proportional to the loss factor of that sprung mass. To increase this bandwidth, a device composed of more than one sprung mass is utilized. The multiplicity of sprung masses with distributed resonance frequencies is the scheme by which a wide frequency band is attained. To keep the undulations in the joint impedance of a set composed of a multiplicity of sprung masses suppressed, the loss factors are rendered larger than the normalized separations between adjacent anti-resonance frequencies. This modal overlap condition, together with the conservation of weight, are central to the design of the device.

20. DISTRIBUTION / AVAILABILITY OF ABSTRACT	21. ABSTRACT SECURITY CLASSIFICATION
☒ UNCLASSIFIED/UNLIMITED ☐ SAME AS RPT. ☐ DTIC USERS	Unclassified

22a. NAME OF RESPONSIBLE INDIVIDUAL	22b. TELEPHONE *(Include Area Code)*	22c. OFFICE SYMBOL
Maidanik, G.	(301) 227-1292	NSWCCD 7030

DD Form 1473, JUN 86 *Previous editions are obsolete.* SECURITY CLASSIFICATION OF THIS PAGE

REPORT DOCUMENTATION PAGE (Continuation Sheet)

19. ABSTRACT (continued)

Two distinct resonance frequency distributions are assigned to corresponding devices and the ranges and parameters that specify the devices are limited to reasonably moderate values; e.g., the useful frequency bandwidth of a device is limited to one-third of its center frequency and the number $(N-1)$ of sprung masses in a device is restricted not to exceed one-score. (For a set composed of a single sprung mass $N=2$ and for a set composed of a multiplicity of sprung masses $N \geq 3$.) In a set employing the first distribution, as (N) is initially increased, an increase in the bandwidth is accompanied by an increase in the joint impedance. As (N) is further increased, the bandwidth and the level of the joint impedance become saturated. In a set incorporating the second distribution, an on-going increase in the bandwidth, as (N) increases, is accompanied by an on-going decrease in the level of the joint impedance. The examination of these and other characteristics in the joint impedance of the sprung masses is provided by data obtained in computer experiments performed on a few selected sets of sprung masses.

When the frequency bandwidth of the device is increased, the amplification or the diminution in the level of the joint impedance, within its viable frequency band, cause the noise control effectiveness of the device to rise or fall, respectively. To assess this potential noise control effectiveness, a noise control criterion is proposed in terms of the overall gain and the normalized overall gain. The latter compares the overall gain of a set of multiple sprung masses with that of a corresponding single sprung mass. These gains assess the noise control that can be mustered by a set of sprung masses in situ. The computer experiments are extended so that several examples of the proposed overall gains, unnormalized and normalized, can be cited.

CONTENTS

ABSTRACT

The design of a wide frequency band neutralizer, vibration absorber and/or structural fuzzy, in the form of multiple sprung masses, is extensively reported in the open literature. The action of the device is reported in terms of the joint point impedance of the sprung masses. This joint impedance is merely the sum over the impedances of the individual sprung masses at the common point to which the device is to be attached to a master structure. The normalized frequency bandwidth of a device composed of a single sprung mass is proportional to the loss factor of that sprung mass. To increase this bandwidth, a device composed of more than one sprung mass is utilized. The multiplicity of sprung masses with distributed resonance frequencies is the scheme by which a wide frequency band is attained. To keep the undulations in the joint impedance of a set composed of a multiplicity of sprung masses suppressed, the loss factors are rendered larger than the normalized separations between adjacent anti-resonance frequencies. This modal overlap condition, together with the conservation of weight, are central to the design of the device. Two distinct resonance frequency distributions are assigned to corresponding devices and the ranges and parameters that specify the devices are limited to reasonably moderate values; e.g., the useful frequency bandwidth of a device is limited to one-third of its center frequency and the number $(N-1)$ of sprung masses in a device is restricted not to exceed one-score. (For a set composed of a single sprung mass $N = 2$ and for a set composed of a multiplicity of sprung masses $N \geq 3$.) In a set employing the first distribution, as (N) is initially increased, an increase in the bandwidth is accompanied by an increase in the joint impedance. As (N) is further increased, the bandwidth and the level of the joint impedance become saturated. In a set incorporating the second distribution, an on-going increase in the bandwidth, as (N) increases, is accompanied by an on-going decrease in the level of the joint impedance. The examination of these and

other characteristics in the joint impedance of the sprung masses is provided by data obtained in computer experiments performed on a few selected sets of sprung masses.

When the frequency bandwidth of the device is increased, the amplification or the diminution in the level of the joint impedance, within its viable frequency band, cause the noise control effectiveness of the device to rise or fall, respectively. To assess this potential noise control effectiveness, a noise control criterion is proposed in terms of the overall gain and the normalized overall gain. The latter compares the overall gain of a set of multiple sprung masses with that of a corresponding single sprung mass. These gains assess the noise control that can be mustered by a set of sprung masses in situ. The computer experiments are extended so that several examples of the proposed overall gains, unnormalized and normalized, can be cited.

I. INTRODUCTION

Ever since structural fuzzies began reverberating within the noise control community, sprung masses, as vibration control devices, have become hot commodities [1-5]. The impedance $Z_j(\omega)$ that the $(j)th$ sprung mass presents to a structure at the "point" (x_j) of attachment is simple enough

$$Z_j(\omega) = i\omega M_j \left[\{1+\eta_j^2 - (\omega/\omega_j)^2\} - i(\omega/\omega_j)^2 \eta_j\right] \bullet$$

$$\left[\{1-(\omega/\omega_j)^2\}^2 + \eta_j^2\right]^{-1} ;$$

$$(\omega_j)^2 = (K_{oj}/M_j) ; \qquad K_j = K_{oj}(1+i\eta_j) , \tag{1}$$

where M_j, ω_j and η_j are the mass, the *resonance frequency*, and the loss factor of that sprung mass. The loss factor is associated with the stiffness K_j of the spring. Consider initially a device of a single sprung mass [3-6]. The resonance frequency of that sprung mass is designated (ω_1), yielding, thereby, a *frequency of resonance*, given by

$$(\omega/\omega_1)^2 = (1+\eta^2) , \tag{2}$$

where (η) is the loss factor associated with that single-sprung mass-device. At and in the vicinity of the frequency of resonance, the impedance $Z(\omega)$ of the sprung mass is resistance controlled and of the approximate form

$$Z(\omega) \simeq (\omega M/\eta) ; \qquad |1-(\omega/\omega_j)^2| \lesssim \eta_j << 1 , \tag{3}$$

where M is the mass of this single-sprung mass-device. The notion that a resistance controlled impedance that is inversely proportional to a loss factor can be presented to a vibrating structure conjures vision of the ultimate noise control device [3,5,6]. One is aware, of course, that in order to increase that resistance controlled impedance, without the penalty of added weight, the loss factor (η) must be kept small, notwithstanding that impedance matching also plays a decisive role in transferring power from one elemental dynamic system to another [7]. But a small (η) implies a narrow-frequency-band device. To overcome this dilemma it is proposed to increase the number of sprung masses at a *point* and to assign to these sprung masses a distribution of resonance frequencies to cover the desired wider frequency bandwidth. To accommodate this proposal several mundane structural models can be devised to enable a multiplicity of sprung masses to be concentrated essentially at a point [1-5]. Sprung masses that perceive a common response at their respective points of attachment can be considered to act at a point. A typical set of sprung masses at a point is sketched in Fig. 1. The expression for the joint impedance that this set of sprung masses presents at a *point* is readily derived; i.e., it is merely the sum of the individual impedances of the sprung masses given by

$$Z_N(\omega) \;=\; \sum_{j=2}^{N} Z_j(\omega) \;; \qquad 2 \;\leq\; j \;\leq\; N \;, \tag{4}$$

and, hence $(N-1)$ is the number of sprung masses in the set [2-5,8]. The overall normalized frequency bandwidth $(\Delta\omega / \omega)$ is related to the highest resonance frequency (ω_2) and the lowest resonance frequency (ω_N) in the set of the sprung masses. Formally,

$$(\Delta\omega / \omega) \;=\; \eta\delta_{2N} + (\Delta\omega / \omega_1)_{N\geq 3}\;(1-\delta_{2N}) \;;\; N \geq 2 \quad , \tag{5}$$

where (ω_1) is a normalizing frequency, (η) is the loss factor and $(\omega_1\eta)$ is the frequency bandwidth of a set composed of a single sprung mass, δ_{2N} is the Kronecker delta in (2) and (N) and $(\Delta\omega / \omega_1)_{N\geq 3}$ is the frequency bandwidth of a set composed of two or more sprung masses. It is noted that the normalized frequency bandwidth of a set composed of two or more sprung masses is

$$(\Delta\omega / \omega_1)_{N\geq 3} = [(\omega_2 - \omega_N) / \omega_1] = \sum_{j=2}^{N-1} [(\omega_j - \omega_{j+1}) / \omega_1] \;\; ; \;\; N \geq 3 \quad . \tag{6}$$

It took a few years, however, to appropriately relate the normalized *on the average* separation $(\delta\omega / \omega)$ between adjacent resonance frequencies and the *on the average* loss factor (η_c) and the normalized *local* separation $(\delta\omega_j / \omega_j)$ between adjacent anti-resonance and the *local* loss factor (η_j), respectively [5,9,10]. These relationships define the condition of modal overlap [11]. The *on the average* condition of modal overlap is expressed in the form

$$\eta_c \geq (\delta\omega / \omega) \; ; \; (\delta\omega / \omega) = (N-2)^{-1} \; [(\omega_2 - \omega_N) / \omega_1] \;\; ; \;\; N \geq 3 \;\; , \tag{7a}$$

where use is made of Eq. (6). On the other hand, the *local* condition of modal overlap is expressed in the form

$$\eta_j \geq (\delta\omega_j / \omega_j) \;\; ; \;\; N \geq 3 \;\; , \tag{7b}$$

and it is noted that the *local* separation $(\delta\omega_j / \omega_j)$ between adjacent anti-resonance frequencies in a set of more than a single sprung mass is

$$(\delta\omega_j / \omega_j) = [(\omega_j^+ - \omega_j^-)/\omega_1](1-\delta_{j2})(1-\delta_{jN}) + 2[(\omega_2 - \omega_2^-)/\omega_1]\delta_{j2}$$

$$+2[(\omega_j^+ - \omega_N)/\omega_N]\delta_{jN} \quad ; \quad 2 \le j \le N \quad ; \quad N \ge 3 \quad , \tag{8}$$

where (ω_j^+) and (ω_j^-) are, respectively, the anti-resonance frequencies on the higher and lower frequency sides of the resonance frequency (ω_j). When the condition of modal overlap is not met, undulations, as a function of frequency, exist. These undulations exist; either *on the average* or *locally*, in the joint impedance $Z_N(\omega)$ of a noise control device composed of a set of sprung masses with $N \ge 3$. The undulations are decreased as the condition of modal overlap is approached; the decreased undulations substantially converge onto steady values as the condition of modal overlap is just reached [12]. [cf. Appendix A.] When the condition of modal overlap is met, the undulations are negligible.

It has been speculated that the mean-values of the undulations assume values that are independent of the loss factors of the individual sprung masses [3, 4, 12]. Therefore, these values are commensurate with the values on which the undulations converge as the overlap condition is just met and beyond, notwithstanding that the overlap condition is a function of the distribution of the resonance frequencies. [cf. Eq. (7).] This speculation is tested herein and the limits on its validity are formulated and revealed. [cf. Appendix A.] Practitioners of noise control do not advocate large fluctuations in the response and, therefore, the condition of modal overlap is usually approached or reached in the design of a set of sprung masses, notwithstanding that an increase in damping, beyond that which just satisfies the modal overlap condition, is held to be detrimental to this design [5]. This notion also is to be tested, and, if possible, quantified, herein. It is within this context that the influence of the damping on the design of a set of sprung masses is investigated. The investigation undertaken is facilitated by relating (η) and $(\delta\omega / \omega)$ to the designed *on the average* loss factor (η_N), and (η) and $(\delta\omega_j / \omega_j)$ to the designed *local* loss factor (η_{Nj}), respectively, in the form

$$\left.\begin{matrix}\eta_N \\ \eta_{Nj}\end{matrix}\right\} = (b)[\eta\delta_{2N} + \left\{\begin{matrix}(\delta\omega / \omega) \\ (\delta\omega_j / \omega_j)\end{matrix}\right\}(1-\delta_{2N})] \quad \begin{matrix}, & \text{(9a)} \\ , & \text{(9b)}\end{matrix}$$

where $(\delta\omega / \omega)$ and $(\delta\omega_j / \omega_j)$ are stated in Eqs. (7a) and (8), respectively, and the overlap factor (b) is defined

$$b = \begin{cases}(1/3), \text{ modal overlap condition is not satisfied}, \\ (2/3), \text{ modal overlap condition is approached}, \\ (3/2), \text{ modal overlap condition is just satisfied}, \\ (2), \text{ modal overlap condition is comfortably satisfied.}\end{cases} \quad (10)$$

The introduction of an auxiliary structure to a master structure often raises the question of weight. An equation of conservation of weight is, therefore, imposed on the design of a set of sprung masses, it is

$$\sum_{j=2}^{N} M_j = (aM_1) \ , \quad (11a)$$

where M_1 is the effective mass of the structure to which the set of sprung masses is to be attached and (a) is the ratio of the total mass M in the set of sprung masses to this effective mass. An acceptable value for (a) is one tenth (10^{-1}). Were the individual masses in the sprung masses assumed to be equal, Eq. (11a) yields

$$M_j = M = (aM_1)[(N-1)]^{-1} \quad , \quad (11b)$$

where M is the mass in each of the sprung masses. [cf. Eq. (3).]

The distribution of the resonance frequencies of the sprung masses in a set may be defined

$$(\omega_j / \omega_1) = [1 + \{2(j-1) - N\}\gamma_N]^{-1/2} \; ; \; \gamma_N(N-1) < 1 \; ; \; 2 \le j \le N \; , \quad (12)$$

with (γ_N) to be related to either the single numerical increment (γ) or (γ_o) in the forms

$$\gamma_N = \begin{cases} (\gamma/2)(N-1)^{-1} & , \quad (13a) \\ \gamma_o & , \quad (13b) \end{cases}$$

respectively, and where the center frequency (ω_1) spans equal numbers of resonance frequencies on the lower and higher frequency ranges. The center frequency (ω_1) is the resonance frequency of a device composed of a single sprung mass, e.g., in Eq. (2), and is also used as a normalizing frequency; e.g., in Eq. (5). It follows, from Eqs. (12), (13a) and (13b), that the difference between the two distributions of resonance frequencies is sustained by the duality of (γ_N). However, if $N = N_o$ and (γ) and (γ_o) are related in the form

$$(\gamma/2)(N_o - 1)^{-1} = \gamma_o \quad , \quad (13c)$$

then, for this value of (N) the value of (γ_N) is degenerate in the two distributions. Therefore, for $N = N_o$ the corresponding parameters and quantities in the two distributions are identical. Substituting Eq. (12) in Eqs. (6), (7a), and (8) one obtains

$$[(\omega_2 - \omega_N)/\omega_1] = [\{1-(N-2)\gamma_N\}^{-1/2} - \{1+(N-2)\gamma_N\}^{-1/2}] \quad , \quad (14a)$$

$$(\delta\omega/\omega) = [\{1-(N-2)\gamma_N\}^{-1/2} - \{1+(N-2)\gamma_N\}^{-1/2}](N-2)^{-1} \quad , \quad (14b)$$

$$(\delta\omega_j / \omega_j) = [\{1 - \gamma_N[1 + \{2(j-1) - N\}\gamma_N]^{-1}\}^{-1/2}$$

$$-\{1 + \gamma_N[1 + \{2(j-1) - N\}\gamma_N]^{-1}\}^{-1/2} \quad , \qquad (14c)$$

respectively, where (γ_N) assumes the one or the other form specified in Eq. (13).

A practical limit needs to be imposed on the frequency bandwidth stated in Eq. (14a). This limit is then imposed in the form

$$[(\omega_2 - \omega_N)/\omega_1] \lesssim 1/3 \;\; ; \;\; N \geq 3 \qquad . \qquad (15)$$

From Eqs. (12), (13), (14a) and (15) one finds that

$$[(\omega_2 - \omega_N)/\omega_1] \simeq [\gamma_N(N-2)] = \left\{ \begin{array}{l} [(\gamma/2)(N-2)(N-1)^{-1}] \\ \\ \gamma_o(N-2) \end{array} \right\} \lesssim (1/3), N \geq 3 \quad \begin{array}{l} , \quad (16a) \\ \\ , \quad (16b) \end{array}$$

where the approximations in Eq. (16) are predicated on the assignment of reasonable parametric limits: $(\gamma \lesssim 0.6)$, $(\gamma_o \lesssim 0.03)$ and $(N \lesssim 20)$. Similarly, from Eqs. (13), (14b) and (15) one finds that

$$(\delta\omega/\omega) \approx \gamma_N = \left\{ \begin{array}{l} [(\gamma/2)(N-1)^{-1}] \\ \\ \gamma_o \end{array} \right\} \quad \begin{array}{l} , \quad (17a) \\ \\ , \quad (17b) \end{array}$$

and from Eqs. (13), (14c) and (15) one finds that

$$(\delta\omega_j / \omega_j) \simeq (\omega_j / \omega_1)^2 \gamma_N$$

$$= \begin{cases} [1 - \{2(j-1) - N\}(\gamma/2)(N-1)^{-1}]^{-1} \quad (\gamma/2)(N-1)^{-1} & , \quad (18a) \\ [1 - \{2(j-1) - N\}\gamma_o]^{-1} \gamma_o & , \quad (18b) \end{cases}$$

where (ω_j / ω_1), and, therefore also $(\omega_j / \omega_1)^2$, are stated in Eq. (12). For a specific numerical increment (γ), Eq. (16a) states that the normalized frequency bandwidth is approximately proportional to $(N-2)\ (N-1)^{-1}$. Compatibly, Eq. (17a) states that the *on the average* normalized separation $(\delta\omega / \omega)$ between adjacent resonance frequencies is approximately proportional to $(N-1)^{-1}$, whereas Eq. (18a) states that the *local* normalized separation $(\delta\omega_j / \omega_j)$ between adjacent anti-resonance frequencies introduces, in addition, a factor of proportionality equal to $(\omega_j / \omega_1)^2$; this factor depends weakly not only on (N), but also on (j). On the other hand, for a specific numerical increment (γ_o), Eq. (16b) states that the normalized frequency bandwidth is approximately proportional to $(N-2)$. Compatibly, Eq. (17b) states that the *on the average* separation $(\delta\omega / \omega)$ is approximately independent of (N); indeed, this normalized quantity is merely approximated by (γ_o). It is conducive then to equate (η) to (γ_o), where (η) is the loss factor of the sprung mass in a set composed of a single member. Here again, Eq. (18b) states that the *local* normalized separations $(\delta\omega_j / \omega_j)$ differs from the corresponding *on the average* separation $(\delta\omega / \omega)$ by a factor of proportionality equal to $(\omega_j / \omega_1)^2$. As just mentioned, in the moderate parametric ranges, this factor harbors a weak, but definite, dependence on both, (N) and (j).

Of course, the masses, the loss factors and the distribution of the resonance frequencies in a set of sprung masses may be defined variously from those stated in Eqs. (9) - (13) and thus yielding results that may be in some variance with those stated in Eqs. (16) - (18). Here, however, the definitions in Eqs. (9) - (13) prove convenient and

varied enough. These definitions are, therefore, adopted as typical examples [10]. Using these adopted definitions, computer experiments are conducted to examine the nature of the joint impedance $Z_N(\omega)$ for a few sets of sprung masses. Of particular interest in this examination are the influences, on the characteristics of this joint impedance, by the variations and the restrictions just presented.

A major question remains: Given that the joint impedance $Z_N(\omega)$ of a set of sprung masses may be designed with specific characteristics, how is the potential noise control effectiveness of this set to be assessed? To answer this question one needs develop a noise control criterion that is based on the performance of a specific set of sprung masses. The performance is to be judged within the context of the response of the structure to which this set is attached; i.e., the master structure. Such a criterion may be expressed in terms of an overall gain $\Gamma_{1N}(\omega)$ defined in the form

$$\Gamma_{1N}(\omega) = |1 + [Z_N(\omega) / Z_1(\omega)]|^2 \quad , \tag{19a}$$

and a normalized overall gain $\overline{\Gamma}_{1N}(\omega)$ defined in the form

$$\overline{\Gamma}_{1N}(\omega) = [\Gamma_{1N}(\omega) / \Gamma_{12}(\omega)] \; ; \quad N \geq 3 \quad , \tag{19b}$$

where $Z_1(\omega)$ is the *point* impedance of the master structure in reference to the *point* of attachment [5,7]. The computer experiments are extended to examine the unnormalized and normalized overall gain $\Gamma_{1N}(\omega)$ and $\overline{\Gamma}_{1N}(\omega)$, respectively, that some selected sets of sprung masses may be able to muster. Two normalized test impedances are assigned in this examination:

$$\{Z_1(\omega)/(\omega_1 M_1)\} = \begin{cases} i(\omega/\omega_1) & , \quad (20a) \\ 1 = (4\sqrt{3})\ \{(mhc_\ell)/(\omega_1 M_1)\} & , \quad (20b) \end{cases}$$

where in Eq. (20a) the point impedance $Z_1(\omega)$ is that of the mass M_1 and in Eq. (20b) the point impedance $Z_1(\omega)$ is that of an unbounded plate and in that plate m, h, and c_ℓ are the mass per unit area, the thickness and the longitudinal speed, respectively [11]. A case in which the master structure itself is a sprung mass is presented extensively under a separate cover [13]. Here it is briefly mentioned that this case is accounted for by

$$\{Z_1(\omega)/(\omega_1 M_1)\} = i(\omega/\omega_1)[(1-(\omega_1/\omega)^2(1+i\eta_1)], \quad (20c)$$

where (ω_1) and (η_1) are the resonance frequency and the loss factor of the master sprung mass, respectively. [cf. Eq. (1).] In contrast to using Eqs. (20a) and (20b), only a cursory use is made of Eq. (20c) in a subsequent computation and display.

II. COMPUTATIONS AND DISPLAYS OF NORMALIZED FREQUENCY BANDWIDTHS AND "ON THE AVERAGE" AND "LOCAL" LOSS FACTORS

The normalized frequency bandwidth $(\Delta\omega / \omega)$, as defined in Eqs. (5), (6), (13) and (14a), is computed and displayed as a function of (N), in Fig. 2. In Fig. 2a, the definition for (γ_N) in Eq. (13a) is imposed, with $\gamma = 0.2$ and 0.4 and 0.6, and $\eta = 0.01,\ 0.02$, and 0.03, respectively. In Fig. 2b the definition for (γ_N) in Eq. (13b) is imposed, with $\gamma_o = \eta = 0.01,\ 0.02$ and 0.03. The increased and subsequent saturation of the normalized frequency bandwidth $(\Delta\omega / \omega)$ with increase in the number $(N-1)$ of sprung masses in the set, is clearly discernible in Fig. 2a. These characteristics in $(\Delta\omega / \omega)$, as a function of (N), are in close agreement with those suggested by Eqs. (5) and (16a). In contrast, the steady increase, without saturation, of the normalized frequency bandwidth $(\Delta\omega / \omega)$ with increase in the number $(N-1)$ of sprung masses in the set, is clearly discernible in Fig. 2b. These characteristics in $(\Delta\omega / \omega)$ are in close agreement with those suggested by Eqs. (5) and (16b).

The *on the average* loss factor (η_N), as defined in Eqs. (9a) and (14b), is computed and displayed as a function of (N), in Fig. 3. In Fig. 3a, the definition for (γ_N) in Eq. (13a) is imposed, with $\gamma = 0.2,\ 0.4$ and 0.6 and with $\eta = 0.01,\ 0.02$ and 0.03, respectively, and in Fig. 3b the definition for (γ_N) in Eq. (13b) is imposed, with $\gamma_o = \eta = 0.01,\ 0.02$ and 0.03. In Fig. 3, the overlap factor (b) is selected to be $(3/2)$. [cf. Eqs. (9) and (10).] It is observed that data in Figs. 3a and 3b of the *on the average* loss factor (η_N) are in close agreement with those suggested by Eqs. (9a) and (17a) and by Eqs. (9a) and (17b), respectively. The *local* loss factor (η_{Nj}), as defined in Eqs. (9b) and (14c), is computed and displayed as a function of (j), with $\gamma = 0.4$ and $\eta = 0.02$, for $N = 6,\ 11$, and 18 in Fig. 4a and with $\gamma_o = \eta = 0.02$, for $N = 6,\ 11$ and 18, in Fig. 4b. Again, in Fig. 4 the overlap factor (b) is selected to be $(3/2)$. [cf.

Eqs. (9) and (10).] The data in Figs. 4a and 4b show close agreement with those predicted in Eqs. (18a) and (18b), respectively. The verifications of these agreements are facilitated by examining Figs. 3 and 5. In Fig. 5, the factor $(\omega_j / \omega_1)^2$ is displayed, as a function of (j), for $N = 6,\ 11$ and 18. In Fig. 5a, (γ_N) is as defined in Eq. (13a) and in Fig. 5b, (γ_N) is as defined in Eq. (13b). The weak, but definite, dependence of $(\omega_j / \omega_1)^2$ on (j) and (N) exhibited in both these figures, is clearly recognized. [cf. Eq. (12).]

The numerical increments (γ) and (γ_o) are selected in Figs. 2-5 to cause the dual distributions of the resonance frequencies to degenerate when $N = 11 = N_o$. Indeed, in Figs. 2-5, the values of two corresponding parameters, each pertaining to the one of the two distributions, are identical for $N = 11$; e.g., the curve for $N = 11$ in Fig. 5a is identical to the curve for $N = 11$ in Fig. 5b.

III. NATURE OF THE IMPEDANCE OF A SET OF SPRUNG MASSES

The impedance $Z_j(\omega)$ of the (j)th sprung mass is stated in Eq. (1). The joint impedance $Z_N(\omega)$ of a set of sprung masses is stated, in terms of the impedances of the individual sprung masses, in Eq. (4). Utilizing Eqs. (9) - (15) to define the quantities and parameters of the set, the normalized joint impedance $\overline{Z}_N(\omega/\omega_1)$ of that set is derived in the form

$$\overline{Z}_N(\omega/\omega_1) = i(\omega/\omega_1)[a/(N-1)]\sum_{j=2}^{N}(1+i\eta_{Nj})\{(1+i\eta_{Nj})$$
$$-(\omega/\omega_1)^2[1+\{2(j-1)-N\}\gamma_N]\}^{-1} \quad ;$$

$$\overline{Z}_N(\omega/\omega_1)=[Z_N(\omega)/(\omega_1 M_1)] \quad , \tag{21}$$

where $(\omega_1 M_1)$ is a normalizing resistance-controlled impedance. Equation (21) may be approximated by replacing the *local* loss factor with the *on the average* loss factor; $\eta_{Nj} \rightarrow \eta_N$, as defined in Eq. (9a). The computations of $\overline{Z}_N(\omega/\omega_1)$, for a set of sprung masses, requires the specifications of: (I) the number (N), indicating that there are $(N-1)$ sprung masses in the set, (II) the mass ratio (a), (III) the duality of the numerical increment (γ_N) and (IV) the corresponding loss factors (η_N) and (η_{Nj}). The natures of the loss factors (η_N) and (η_{Nj}) have just been investigated in the preceding section. [cf. Eq. (9) and Figs. 3 and 4.] The displays of the computations of the normalized joint impedance $\overline{Z}_N(\omega/\omega_1)$ are presented in terms of Re $\{\overline{Z}_N(\omega/\omega_1)\}$, Im $\{\overline{Z}_N(\omega/\omega_1)\}$ and $|\overline{Z}_N(\omega/\omega_1)|$, as functions of the normalized frequency (ω/ω_1). These three normalized quantities for a set composed of a single sprung mass are depicted in Figs. 6a, 6b and 6c, respectively. Each sub-figure features three curves

pertaining to three values of the overlap factor (b); the light curves are for $b = (1/3)$, the darker curves are for $b = (2/3)$ and the darkest curves are for $b = (3/2)$. [cf. Eq. (10).] In the annals of a responding single sprung mass, Fig. 6 is self explanatory and needs no special commentary. Figure 6 is repeated for a set composed of ten sprung masses; i.e., $N = 11$, in Figs. 7 and 8. The numerical increments (γ) and (γ_o) are selected to be 0.4 and 0.02, respectively, so that $N_o = 11$, where N_o is defined in Eq. (13c). Therefore, Figs. 7 and 8 simultaneously pertain to both distributions of the resonance frequencies. In Fig. 7, the *on the average* loss factors, as depicted in Fig. 3, are appropriately used. In Fig. 8, the *local* loss factors, as depicted in Fig. 4, are also appropriately used. Again, in each figure; e.g., in Fig. 7, the three quantities are presented as functions of the normalized frequency (ω/ω_1); e.g., Figs. 7a, 7b and 7c depict $\text{Re}\{\bar{Z}_N(\omega/\omega_1)\}$, $\text{Im}\{\bar{Z}_N(\omega/\omega_1)\}$ and $|\bar{Z}_N(\omega/\omega_1)|$, respectively, as functions of the normalized frequency (ω/ω_1). [cf. Fig. 6a, 6b and 6c, respectively.] Finally, each sub-figure; e.g., Fig. 7a, features three curves pertaining to three values of the overlap factor (b); as in Fig. 6, the light curves are for $b = (1/3)$, the darker curves are for $b = (2/3)$ and the darkest curves are for $b = (3/2)$. [cf. Eq. (10).] Under careful scrutiny it is observed that Fig. 7, which employs the *on the average* loss factor, yields the less symmetric (uniform) undulations and, naturally, Fig. 8, which employs the *local* loss factor, yields undulations that are fairly symmetric (uniform). (The symmetry is about the center frequency (ω_1).) It is noted, however, that in the range displayed in these figures, the difference between the two forms of loss factors; the *on the average* and *locally* based loss factors, is at best a factor of two. From a noise control view a design that calls for the control of loss factors to better than a factor of two (2) is impractical. In that sense then, the comparison for differences between Figs. 7 and 8 is merely of an academic interest [5]. In this connection, the undulated values, in the normalized joint impedance, converge onto a common curve, as the undulations are suppressed by the increase in the loss factors via an increase in the overlap factor (b). The convergence is

just complete as the overlap factor (b) reaches the neutral value of $(3/2)$. For values of (b) that are less than $(3/2)$, i.e., when $(b) < (3/2)$, it emerges in these figures, that the common curve is substantially coincident with all the mean-values curves of the undulations. This convergence then defines the manner by which the undulations can be meaningfully averaged [12]. [cf. Appendix A.]

A gross variation on the theme may now be introduced and the influence that this variation may have on the absolute values of the normalized joint impedance $|\bar{Z}_N(\omega/\omega_1)|$ is investigated. The investigation is conducted in terms of Fig. 9. This figure repeat Fig. 8c except that the overlap factor (b) is changed from the three standard values of $(1/3)$, $(2/3)$ and $(3/2)$ to the four values of $(3/2)$, (2), (4) and (8), respectively. The erosion of the level $|\bar{Z}_N(\omega/\omega_1)|$ when the overlap condition is overly satisfied is clearly discernible in Fig. 9. Indeed, in the light of Fig. 9, one may deduce that the darkest curves in Figs. 7 and 8, which pertain to an overlap factor $(b) = (3/2)$, already bear tinges of erosion and hence the marginal deviations of these curves from strictly mean-value curves [12]. The erosion is initially most pronounced at the edges of the frequency band. [cf. Appendix A for more details.]

Finally, in Fig. 10, the absolute values of the normalized joint impedance, i.e., the values of $|\bar{Z}_N(\omega/\omega_1)|$, are presented as a function of (ω/ω_1) for a number of (N)'s; $N = 1, 3, 4, 6, 8, 11, 14$ and 18, and for an overlap factor of (b) equal to $(3/2)$. In Fig. 10a (γ_N) takes the definition in Eq. (13a) and in Fig. 10b (γ_N) takes the definition in Eq. (13b). Again, (γ) and (γ_o) are selected as 0.4 and 0.02, respectively, so that (N_o) as defined in Eq. (13c) is eleven (11). The increase of the frequency bandwidths and the accompanied increase in the mean-levels of $|\bar{Z}_N(\omega/\omega_1)|$ within these frequency bands, as (N) is initially increased, and then the saturation of both, with further increases in (N), is clearly exhibited in Fig. 10a. On the other hand, the continuous broadening of the frequency bandwidths and the accompanied diminishing in the mean-levels of $|\bar{Z}_N(\omega/\omega_1)|$ within these frequency bands, as (N) increases, emerges loud and clear in

Fig. 10b. Nonetheless, in spite of this fundamental difference in behavior, the curve in Fig. 10a for $N = 11 = N_o$ and the corresponding curve in Fig. 10b are identical as dictated by Eq. (13c).

IV. OVERALL GAIN OF A SET OF SPRUNG MASSES ATTACHED TO A MASTER STRUCTURE

The overall gain $\Gamma_{1N}(\omega)$ and the normalized overall gain $\overline{\Gamma}_{1N}(\omega)$ for a set of sprung masses are stated in Eq. (19). Utilizing Eqs. (20) and (21) the overall gain may be stated in the form.

$$\Gamma_{1N}(\omega/\omega_1) = \left|1+[\overline{Z}_N(\omega/\omega_1)/\overline{Z}_1(\omega/\omega_1)]\right|^2 \quad ; \quad N \geq 3 \quad , \qquad (22a)$$

and the corresponding normalized overall gain may be stated in the form

$$\overline{\Gamma}_{1N}(\omega/\omega_1) = [\Gamma_{1N}(\omega/\omega_1)/\Gamma_{12}(\omega/\omega_1)] \quad ; \quad N \geq 3 \quad , \qquad (22b)$$

where the normalized point impedance $\overline{Z}_1(\omega/\omega_1)$ in the master structure may be cast in the form

$$\overline{Z}_1(\omega/\omega_1) = \left\{ \begin{array}{c} i(\omega/\omega_1) \\ 1 \\ i(\omega/\omega_1)[1-(\omega_1/\omega)^2(1+i\eta_1)] \end{array} \right\} \begin{array}{l} , \quad (23a) \\ , \quad (23b) \\ . \quad (23c) \end{array}$$

It is recognized that an overall gain $\Gamma_{1N}(\omega/\omega_1)$ that is unity is gainless, less than unity is ineffective and greater than unity is effective, gaining a beneficial noise reduction. Clearly, given an adequate frequency bandwidth, the more the overall gain exceeds unity in that frequency band the better is the insitu performance of the referenced noise control device. On the other hand, a normalized overall gain $\overline{\Gamma}_{1N}(\omega/\omega_1)$ that is unity is neutral, less than unity is deficient and greater than unity is efficient. In an efficient region, a set of multiple

sprung masses performs more effectively than a corresponding single sprung mass. Indeed, the employment of a multiplicity of sprung masses is an attempt to widen the frequency bandwidth and sustain, on balance, an efficient normalized overall gain within that wider frequency band. The normalized overall gain $\overline{\Gamma}_{1N}(\omega / \omega_1)$ furnishes information with regard to this balance. Figures 11a and 11b and Figs. 12a and 12b depict the overall gain, as a function of (ω / ω_1), derived by converting data presented in Fig. 10a and Fig. 10b, ala' Eq. (22a), under the guidance of Eqs. (23a) and (23b), respectively. Similarly, Figs. 11d and 11e and Figs. 12c and 12d depict the normalized overall gain as a function of (ω / ω_1) derived by converting data presented in Fig. 10a and Fig. 10b, ala' Eq. (22b), under the guidance of Eqs. (23a) and (23b), respectively. The identical darkest curves, in Figs. 11a and 12a and in Figs. 11b and 12b pertain to a set consisting of a single sprung mass that is attached to a point on a master structure. The test impedances at this attachment point are as stated in Eqs. (23a) and (23b), respectively. These identical darkest curves in Figs. 11a and 12a exhibit a narrow ridge in the overall gain. That ridge peaks at $(\omega / \omega_1) = 1$ and is accompanied by a nadir at a slightly higher frequency. At the peak the overall gain is effective; at the nadir it is ineffective. Analogously, in Figs. 11b and 12b, the ridge, in the identical darkest curves, is also narrow and it peaks at $(\omega / \omega_1) = 1$. However, at and in the vicinity of $(\omega / \omega_1) = 1$, the peak stands alone. At the peak the overall gain is effective; outside the narrow band, which is centered on the peak, the overall gain bottoms on unity. Thus, for a set consisting of a single sprung mass, Figs. 11 and 12 readily exhibit an effective overall gain. However, this effectiveness is confined to a narrow frequency band. Indeed, the narrowness of the frequency band in which the effective overall gain lies; i.e., the darkest curves in Figs. 11 and 12, is the reason for proposing a device incorporating a set composed of a multiplicity of sprung masses [1-5]. A query arises in this connection: Is such a proposal viable in the sense that an extended bandwidth can be attained with an overall gain that is effective in that wider frequency band? To prepare the answer to this question, the data presented in

Figs. 11 and 12 are more extensively studied. With an increase in (N), Fig 11a exhibits a broadening of the frequency bandwidths, a shift in the peaks to lower frequencies and an enhancement in the effectiveness. It is also observed that as (N) increases, the ineffectiveness in the overall gain become more severe and the nadirs are shifted to higher frequencies. However, the broadening of the bandwidths, the frequency shifts of the peaks and the nadirs, and the enhancement in the effectiveness and the ineffectiveness all saturate in Fig. 11a with a further increase in (N). This saturation renders the changes with the increase in (N) largely insignificant once (N) exceeds the critical number (N_c). Adding complications, such as an increase in the number of sprung masses, without definitive benefits is not a good design procedure. Similarly, with increases in (N), Fig. 12a exhibits a continuous broadening of the frequency bandwidths, a shift in the frequencies of the peaks and the nadirs and a reduction in the effectiveness and the ineffectiveness. The continuity of these changes with increases in (N) cannot be beneficially maintained beyond the critical number (N_c); when (N) increases beyond (N_c), the reduced effectiveness in the overall gain is rendered unacceptable. In summary, the overall gain presented in Figs. 11a and 12a for $(N_c \geq N \geq 3)$ cannot be considered a major improvement over that for a set of a single sprung mass for which $N = 2$. Thus, although ostensibly the absolute values of the normalized joint impedance, as displayed in Figs. 10a and 10b, hold a promise for an effective overall gain, that promise is largely evaporated in Figs. 11a and 12a. The normalized test impedance that is assigned to Figs. 11a and 12a is that stated in Eq. (23a); namely, $\overline{Z}_1(\omega/\omega_1) = i(\omega/\omega_1)$. On the other hand, Figs. 11b and 12b show that, as (N) increases, the frequency bandwidths become wider and remain centered about $(\omega/\omega_1) = 1$. These figures also show that the overall gain levels bottom on unity and, therefore, the overall gain is never ineffective. The saturation of the frequency bandwidth and levels in Fig. 11b, again defines a critical number (N_c); a larger number of sprung masses than $(N_c - 1)$ contributes little to the overall gain in both, frequency bandwidth and level. It appears, from Fig. 11b, that the

saturated frequency bandwidth and the saturated level in that frequency band relate inversely to each other. This statement is supported and is vividly illustrated in Fig. 11c. In this figure the value of the numerical increment (γ) is set equal to 0.2, while in Fig. 11b it is equal to the standard value of 0.4. In Fig. 11c, as compared with Fig. 11b, a reduction in the saturated frequency bandwidth is traded for an increase in the saturated level.

In Fig. 12b, one finds that the continuous broadening of the frequency bandwidths is accompanied by a reduction in the levels of the overall gain in that frequency band. Again, this inverse relationship between a frequency bandwidth and a corresponding level defines the critical number (N_c). When (N) increases beyond (N_c), the resulting reduction in level (effectiveness) renders the level unacceptable. Moreover, since (γ_o), in Fig. 12b is retained at the standard value of 0.02, and the standard value of 0.4 for (γ) is halved to 0.2 in Fig. 11c, Eq. (13c) dictates that the corresponding curves, in these two figures, for $N = 6 = N_o$ are identical.

In summary, and in contrast to Figs. 11a and 12a, the overall gain presented in Figs. 11b and 12b for $(N_c \geq N \geq 3)$ indicates an improvement over the overall gain pertaining to a set of a single sprung mass for which $(N = 2)$. In these figures, the latter is depicted by the darkest curves. Thus, the promise that may be held by the absolute values of the normalized joint impedance, as presented in Figs. 10a and 10b, materializes, in part, in Figs. 11b and 12b. In these figures, the normalized test impedance $\overline{Z}_1(\omega / \omega_1)$ on the master structure is as stated in Eq. (23b); namely, $\overline{Z}_1(\omega / \omega_1) = 1$.

How crucial is the role of $\overline{Z}_1(\omega / \omega_1)$ in the determination of the noise control benefits that can be accrued from a device incorporating a multiplicity of sprung masses? In part, the answer to this question has already been advanced; the noise control benefits accrued in Figs. 11b and 12b are superior to those in Figs. 11a and 12a. To enrich the answer, yet two more figures, Fig. 13a and 13b, are displayed. These figures use data presented in Fig. 10b together with the normalized test impedance stated in Eq. (23c) to

compute the overall gain $\Gamma_{1N}(\omega/\omega_1)$ as a function of the normalized frequency (ω/ω_1). In Fig. 13a the loss factor (η_1) is set equal to 10^{-1} and in Fig. 13b to 10^{-2}. Figures 13a and 13b exhibit more extreme regions of effectiveness and ineffectiveness than the corresponding regions in Fig. 12b. Moreover, the regions in Fig. 13b are more extreme than in Fig. 13a. Therefore, the loss factor (η_1) of the master sprung mass, as well as the fact that the master structure is a sprung mass, significantly influences the levels of these extremes.

It is advantageous, at this stage, to solicit the information that may lie in Figs. 11d and 11e and Figs. 12c and 12d; these figures display the normalized overall gain $\overline{\Gamma}_{1N}(\omega/\omega_1)$ as a function of the normalized frequency (ω/ω_1). The information in these figures may be judged in the light of Figs. 11a and 11b and Figs. 12a and 12b, respectively. The effectiveness and the ineffectiveness in Fig. 11a turns, understandably, into a deficiency and an efficiency in Fig. 11d. Moreover, from Fig. 11d, it is apparent that the gain in efficiency over a wider frequency band hardly materialized. Similarly, the high effectiveness of the single sprung mass in Fig. 11b is manifested as a deep deficiency in Fig. 11e. Further, from Fig. 11e, it is observed that the gain in efficiency over a wider frequency band barely materialized. From Figs. 12a and 12c and Figs. 12b and 12d, it is concluded that with respect to the gain in efficiency over a wider frequency band, these pairs of figures do not fare much better than do Figs. 11a and 11d and Figs. 11b and 11e, respectively. The situation is improved in Figs. 13a and 13c and Figs. 13b and 13d. Figures 13c and 13d display the normalized overall gain $\overline{\Gamma}_{1N}(\omega/\omega_1)$ that correspond to the overall gain $\Gamma_{1N}(\omega/\omega_1)$ that is displayed in Figs. 13a and 13b, respectively. From Figs. 13a and 13c and Figs. 13b and 13d, it is concluded that, with respect to the gain in efficiency over a wider frequency band, these pairs of figures fare a little better than do Figs. 12b and 12d. Which pairs of figures; either Figs. 13a and 13c or Figs. 13b and 13d, describe a more viable noise control device is a design problem that needs to be tackled by more expanded consideration; e.g., how much of a deficiency can be tolerated at

and in the vicinity of $(\omega / \omega_1) = 1$ and yet satisfy a viable noise control goal? In addition, were a noise control goal to be proposed, how significant to this proposal are the efficiencies on either side of the immediate frequency region defined by $(\omega / \omega_1) \simeq 1$? Moreover, the deficiencies and efficiencies in Figs. 13c and 13d exceed the corresponding ones in Fig. 12d. How significant to the proposal are such variations in efficiencies? Using Eqs. 11-13, the answers to these kind of questions are largely inconclusive, if not confusing. In spite of these observations, one can, nonetheless and with caution, develop a few criteria to assist with the design of a viable noise control device prior to the specifications of its insitu attachment. These criteria in the design process merely constitute necessary conditions. Often necessary conditions are a mouthful, and thus, the remaining part of this report is devoted to the development of such criteria. The sufficiency of these conditions need await the specifications of the test impedance of the master structure, which in the coming development is merely neglected. One need not, however, ignore that in the final analysis the *insitu performance* of the *device* is all that really counts and, for this purpose, a knowledge of this test impedance is an essential ingredient in the final design. [5].

V. CRITERIA OF PROMISE FOR A NOISE CONTROL DEVICE INCORPORATING A SET OF SPRUNG MASSES

The noise control viability of a device composed of a single sprung mass may be assessed in terms of its normalized impedance $\bar{Z}_2(1)$ at resonance and its normalized bandwidth $(\Delta\omega / \omega)_2$. Both of these quantities are readily stated in the form

$$\bar{Z}_2(1) = (a / b\eta) \quad ; \quad (\Delta\omega / \omega)_2 = (b\eta) \tag{24}$$

where (η) and (b) are defined in Eqs. (9) and (10). A *criterion of viability* for this device may be stated in the form

$$\bar{Z}_2(1) >> 1 \quad ; \quad (b\eta) << (a) \quad . \tag{25}$$

The device, as discussed earlier, suffers from a lack of adequate frequency bandwidth. That sufferance may be accounted for by defining a *parameter of promise* $C_2(b)$ defined by the product of the normalized impedance at resonance and the corresponding frequency bandwidth [5]. From Eqs. (24) and (25) one obtains

$$C_2(b) = \bar{Z}_2(1)(\Delta\omega / \omega)_2 = (a) \quad . \tag{26}$$

If a device incorporating a multiplicity of sprung masses is designed with the intention of deriving a wider frequency band, using Eqs. (6) and (16) that intention can be qualified in the form

$$(\Delta\omega / \omega_1)_{N\geq 3} = [(\omega_2 - \omega_N) / \omega_1] \simeq [(N-2)\gamma_N] > (b\eta) \; ; \; N \geq 3. \tag{27}$$

A *criterion of viability* for this device is cast in terms of the average normalized level of the joint impedance $\langle | \bar{Z}_c(\omega / \omega_1) | \rangle$, where the angular brackets indicate mean-value averaging over the frequency band defined in Eq. (27). The criterion demands that this quantity exceeds unity in that frequency bandwidth; namely

$$\langle | \bar{Z}_N(\omega / \omega_1) | \rangle \gtrsim 1 \quad ; \quad N \geq 3 \quad , \tag{28a}$$

for only under this condition can one necessarily ensure the potential viability of the overall gain for this device. Following the suggestion made in Eq. (24), one obtains from Eqs. (9), (18) and (21) that

$$\bar{Z}_N(1) \approx i[a/(N-1)\gamma_N] \sum_{j=2}^{N} \{(ib)(\omega_j / \omega_1)^2 + (N+2-2j)\}^{-1} \quad ;$$

$$N \geq 3 \quad , \tag{29a}$$

which can be further approximated in the form

$$\bar{Z}_N(1) \approx [a/(N-1)\gamma_N] A_N(b) \quad ; \quad N \geq 3 \quad , \tag{29b}$$

where

$$A_N(b) = \sum_{j=2}^{N} i\{(ib) + (N+2-2j)\}^{-1} \quad ; \quad N \geq 3 \quad . \tag{30a}$$

The quantity $A_N(b)$ is real and, provided the overlap factor (b) is about $(3/2)$, it is of the order of unity. [cf. Appendix A.] This statement, with regards to $A_N(b)$, is illustrated

in Fig. 14a; in this figure $A_N(b)$ is displayed as a function of (N) for $(b) = (1/3)$, $(2/3)$, $(3/2)$ and (4). The undulations in $A_N(b)$ when (b) is less than $(3/2)$ is obvious in Fig. 14a. The undulations are between the maxim at resonance for the even (N)'s and the minima at anti-resonance for the odd (N)'s when the overlap condition is not met. When this condition is met, i.e., when (b) exceeds $(3/2)$, the undulations, as usual, are suppressed. The erosion that sets into $A_N(b)$ when the conditions of modal overlap is overly satisfied; $(b) > (3/2)$, is clearly discernible in Fig. 14a. [cf. Fig. 9.] To satisfy a mean-value averaging for the *criterion of viability*, stated in Eq. (28a), one introduces an undulation-free construct into Eq. (29b) in the form

$$\langle | \bar{Z}_N(\omega/\omega_1) | \rangle \simeq [a/(N-1)\gamma_N]\bar{A}_N(b) \geq 1 \ ; \ N \geq 3 \ , \tag{28b}$$

where

$$\bar{A}_N(b) = [A_N(b)A_{N+1}(b)]^{1/2} \ . \tag{30b}$$

The quantity $\bar{A}_N(b)$ is real and is free of undulations in the sense that it is geometrically averaged to determine a mean-value for $\langle | Z_N(\omega/\omega_1) | \rangle$ [12]. The quantity $\bar{A}_N(b)$ as a function of (N) for $(b) = (1/3)$, $(2/3)$, $(3/2)$ and (4) is presented in Fig 14b. Figures 14a and 14b indicate that both $A_N(b)$ and $\bar{A}_N(b)$ are functions of both (N) and (b). Also indicated is the convergence of both functions onto an asymptotic value of $(\pi/2)$ as (N) increases; the convergence is more rapid in (N) the smaller is the overlap factor (b). [cf. Appendix A.] The convergence of $A_N(b)$ is undulated; naturally the stroke of the undulations is larger the smaller is (b). On the other hand, the convergence of $\bar{A}_N(b)$ is undulation-free by construction. [cf. Eq. (30b).] The erosion is a manifest that the range of (N) in Figs. 14a and 14b is insufficient for $A_N(b)$ and $\bar{A}_N(b)$ to converge onto $(\pi/2)$ when (b) exceeds $(3/2)$ and beyond. [cf. Appendix A.]

Again, one may define and evaluate, from Eqs. (27) and (28b), a *parameter of promise* $C_N(b)$ in terms of the product of the average joint impedance $\langle | Z_N(\omega/\omega_1) | \rangle$ and the bandwidth $(\Delta\omega/\omega_1)_{N\geq 3}$; namely

$$C_N(b) = \langle | \bar{Z}_N(\omega/\omega_1) | \rangle (\Delta\omega/\omega_1)_{N\geq 3} \simeq [a/(N-1)](N-2)\bar{A}_N(b); N \geq 3 \quad , \tag{31}$$

which is independent of (γ_N) and, therefore, of the distribution of the resonance frequencies. A *criterion of promise* $\bar{C}_N(b)$ may then be defined as the ratio of the *parameter of promise* $C_N(b)$ of a noise control device incorporating $(N-1)$ sprung masses to the *parameter of promise* $C_2(b)$ of a noise control device incorporating but a single sprung mass [5]. From Eqs. (26) and (31) the *criterion of promise* is derived

$$\bar{C}_N(b) = [C_N(b)/C_2(b)] \simeq (N-1)^{-1}(N-2)\bar{A}_N(b) \quad ; \quad N \geq 3 \quad . \tag{32}$$

The larger $\bar{C}_N(b)$, the more the promise that the device may potentially hold. [A similar quantity, defined as the "gain bandwidth product," was presented in Reference 5. In this reference a minor variation on the second distribution of resonance frequencies was employed.] The *criterion of promise* $\bar{C}_N(b)$ is computed as a function of (N) for $(b) = (1/3), (2/3), (3/2)$ and (4); the results of these computations are displayed in Fig. 14c. It is noted that the undulations that beset Fig. 14a are suppressed, as intended, in Fig. 14c. Moreover, the erosion that sets in when the conditions of modal overlap is overly satisfied; i.e., when (b) exceeds $(3/2)$, is clearly exhibited in Fig. 14c [cf. Figs. 9a, 9b and 13a.] Figure 14c shows that $\bar{C}_N(b)$ saturates; this saturation defines a critical number (N_c) for (N). Most of the promised benefits are accrued for a device incorporating $(N_c - 1)$ sprung masses; a demand for a larger number of sprung masses becomes an excessive design sophistication. Finally, as discussed earlier, the insitu

viability of the devices can be ascertained only in terms of the overall gain $\Gamma_{1N}(\omega / \omega_1)$, stated in Eq. (22). The *criterion of viability,* as stated in Eq. (28), and the *criterion of promise,* as stated in Eq. (32), are merely necessary conditions; they are, by no means, sufficient conditions to ensure the viability of the overall gain of a noise control device incorporating a multiplicity of sprung masses. The viability of the overall gain is crucially dependent on the normalized point impedance that the noise control device perceives in the host structure--the master structure--to which it is attached. Moreover, to ascertain the viability of the noise control device, the characteristics of the device need to be described in a manner that facilitates the assessment of the true achievement that can be mustered by the device, e.g., the complex values of the joint impedance perceived by the master structure as compared with the absolute values of this quantity [5].

APPENDIX A

A dynamic quantity (or a *measure);* e.g., either $\overline{Z}_N(\omega/\omega_1)$ or $A_N(b)$, is formulated with the intention of describing the characteristics in the dynamic behavior of a set of sprung masses. These characteristic are revealed by appropriately expressing and displaying these quantities; e.g., $\overline{Z}_N(\omega/\omega_1)$ is depicted as a function of (ω/ω_1) and $A_N(b)$ is depicted as a function of (N). Often the characteristics of one quantity are related to the characteristics of another. Indeed, $A_N(b)$ is a factor in $\overline{Z}_N(\omega/\omega_1)$ when the latter is evaluated at $(\omega/\omega_1) = 1$. [cf. Eq. (29).] It is not surprising then that undulations are clearly discernible in the displays of both these quantities when the overlap factor (b) is less than $(3/2)$. Moreover, the excursions in the undulations in both quantities are more prominent the smaller this factor is. Again, in both quantities the undulations are suppressed into steadily monotonic values when the overlap factor (b) exceeds $(3/2)$. The undulations in both quantities can be suppressed by special constructs so than even when $[b < (3/2)]$ the constructed quantities exhibit values that are steadily monotonic. In this vein, a proper construct is one for which the steadily monotonic values largely coincide with the mean-values of the undulations in the original quantity and the undulation-free values in the original quantity substantially coincide with those in the construct [12]. Thus, the constructed quantity $\overline{A}_N(b)$, stated in Eq. (30b) and displayed in Fig. 14b, is a proper construct of the original quantity $A_N(b)$, stated in Eq. (30a) and displayed in Fig. 14a. Briefly stated, $\overline{A}_N(b)$ is a proper mean-values counterpart of $A_N(b)$. A question arises: are all mean-values the same; i.e., is $\overline{A}_N(b)$ independent of (b)? The answer to this question is of particular interest to this Appendix. In part, the answer to this question is cavalierly given in the text. In the range of moderate parametric values, the figures in the text indicate that although for large overlap factors $[b > (3/2)]$ the values of $A_N(b)$ and $\overline{A}_N(b)$ are the same, the values are eroded in the

sense that these values lie below the mean-values of $\bar{A}_N(b)$ and the values of $\bar{A}_N(b)$ that pertain to the small overlap factors $[b < (3/2)]$. The erosion is particularly severe for the smaller values of (N) and the larger values of (b). On the other hand, for small, but different, overlap factors $[b \lesssim (3/2)]$, the mean-values of the undulations in $A_N(b)$, as well as the corresponding values of the undulation-free construct $\bar{A}_N(b)$, are closer to each other and this closeness is the cozier the larger the values of (N) are. The quantification of these observations is also of particular interest to this Appendix.

It is conducive at this stage to select an alternative implementation of $\bar{A}_N(b)$ to that stated in Eq. (30b). In this alternative implementation one defines

$$A_{(N\pm 1/2)}(b) = (i/2)\sum_{j=2}^{N}[\{(ib)+(N+1-2j)\}^{-1} + \{(ib)+(N+3-2j)\}^{-1}]$$

$$= \sum_{j=1}^{N}(i\,\varepsilon_{1,j}\;\varepsilon_{N,j})\{(ib)+\{(ib)+(N+1-2j)\}^{-1} \;;\; N \geq 3 \;, \qquad \text{(A1)}$$

where

$$\varepsilon_{r,j} = \begin{cases} (1/2) \;;\; r = j \\ 1 \;\;\;\; ;\; r \neq j \end{cases} \;. \qquad \text{(A2)}$$

The function $A_{(N\pm 1/2)}(b)$ is computed and displayed as a function of (N), for $(b) = (1/3),\ (2/3),\ (3/2)$ and (4), in Fig. A1. The similarity between $A_N(b)$, shown in Fig. 14a, and $A_{(N\pm 1/2)}(b)$, shown in Fig. A1, is striking; they are substantially the same except for a displacement of unity with respect to (N). [cf. $A_{(N+1)}(b)$ in Eq. (30a), which is also displaced from $A_N(b)$ by unity with respect to (N).] The function $A_{(N\pm 1/2)}(b)$ may be employed to define $\bar{A}_N(b)$ in the alternative form

$$\bar{A}_N(b) \;=\; [A_N(b)A_{(N\pm 1/2)}(b)]^{1/2} \quad ; \quad N \geq 3 \quad , \tag{A3}$$

where the explicit expression for $A_N(b)$ is stated in Eq. (30a). [cf. Eqs. (28) and (29).] The quantity $\bar{A}_N(b)$, as stated in Eq. (A3), is depicted as a function of (N) in Fig. A2; the overlap factor (b) is set in this figure equal to $(1/3)$, $(2/3)$, $(3/2)$ and (4). The substantial identity of Fig. A2 with Fig. 14b is clearly discernible. To identify and address the particular interest of the Appendix, it is required to make explicit the dependency of $\bar{A}_N(b)$, as stated in Eq. (A3), on the overlap factor (b) and on the subscript (N). In attempting to ascertain this dependency it is convenient to distinguish between an (N) that is *even* and an (N)that is *odd*. Employing Eqs. (30a), (A1) and (A3), one readily manipulates and derives

$$\bar{A}_N(b) = [\sum_{j=2}^{(N+2)/2} \varepsilon_{(N+2)/2,j}\,(2b^2)\{b^2 + (N+2-2j)^2\}^{-1}]^{1/2}$$

$$\bullet\; [\sum_{j=1}^{N/2} \varepsilon_{ij}(b^2 + N + 1 - 2j)^2\}^{-1}]^{1/2} \quad , \tag{A4}$$

for an (N) that is *even*, and

$$\bar{A}_N(b) = [\sum_{j=1}^{(N+1)/2} \varepsilon_{1,j}\;\varepsilon_{(N+1)/2,j}\,(2b^2)\{b^2 + (N+1-2j)^2\}^{-1}]^{1/2}$$

$$\bullet\; [\sum_{j=2}^{(N+1)/2} 2\{b^2 + (N+2-2j)^2\}^{-1}]^{1/2} \quad , \tag{A5}$$

for an (N) that is *odd*, where $\varepsilon_{r,j}$ is defined in Eq. (A2). In "long hand", Eqs. (A4) and (A5) assume the forms

$$\overline{A}_N(b) = [1 + 2b^2\{(b^2+4)^{-1} + (b^2+16)^{-1} + \ldots + (b^2+[N-2]^2)^{-1}\}]^{1/2}$$

$$\bullet\ [2\{(b^2+1)^{-1} + (b^2+9)^{-1} + \ldots + (1/2)(b^2+[N-1]^2)^{-1}\}]^{1/2} \quad , \qquad \text{(A6)}$$

$$\overline{A}_N(b) = [1 + 2b^2\{(b^2+4)^{-1} + (b^2+16)^{-1} + \ldots + (1/2)(b^2+[(N-1)]^2)^{-1}\}]^{1/2}$$

$$\bullet\ [2\{(b^2+1)^{-1} + (b^2+9)^{-1} + \ldots + (b^2+[N-2]^2)^{-1}\}]^{1/2} \quad , \qquad \text{(A7)}$$

respectively. For a large enough (N), and independently of whether (N) is *even* or *odd,* one may derive from Eqs. (A6) and (A7) the asymptotic evaluation

$$\overline{A}_N(b) \rightarrow (\pi/2) \ ; \ N >> (\pi b/2) \ ; \ N \geq 3 \quad . \qquad \text{(A8)}$$

The validity of Eq. (A8) is predicated on (b), but once this equation is validated, $\overline{A}_N(b)$ is independent of (b) [14]. As (N) satisfies the second of Eq. (A8), the asymptotic convergence of the curves, in Figs. 14b and A2, is clearly explained by the first of Eq. (A8). A heuristic expression for $\overline{A}_N(b)$ that seems to embody Eq. (A8) and that conforms to the data presented in Figs. 14b and A2, may be cast in the form

$$\overline{A}_N(b) \simeq (\pi/2)\exp[-g(N)f(b)] \ ; \ N \geq 3 \quad , \qquad \text{(A9)}$$

where

$$g(N) = (2N-1)[2(N-1)N]^{-1} \underset{N>>3}{\rightarrow} (1/N) \quad , \tag{A10a}$$

$$f(b) = (2)^{-1/2}[10^{-1} + (b)] \quad . \tag{A10b}$$

The conformity of Eq. (A9) to Eqs. (A6) and (A7) is depicted in Fig. A2; the conformity is sufficiently tight. Equation (A9) is simple enough and yet it serves and satisfies the purpose for which the Appendix is brought to bear. Some of these bears are discussed in the introduction to this Appendix. Thus, for example, relying on Eq. (A9) one may assert that the undulations in Figs. 14a and A1, maintain largely the same mean-values, within 10% range of $(\pi/2)$, provided

$$g(N)f(3/2) \lesssim 10^{-1} \quad ; \quad [g(N_c)]^{-1} \simeq 11 \simeq N_c \quad , \tag{A11a}$$

or within 20% range of $(\pi/2)$ provided

$$g(N)f(3/2) \lesssim 2x10^{-1} \quad ; \quad [g(N_c)]^{-1} \simeq 5 \simeq N_c \quad , \tag{A11b}$$

where the data presented in Fig. A2 is utilized, and (N_c) is the critical number of (N) as defined and discussed in the text. Other features in Figs. 14a and A1, and in other figures in the text, can be explained and accounted for using Eq. (A9). In particular, Eq. (A9) is decisively keyed to deciphering the role played by the mean-values, by the erosions in the values of *measures* and by the critical number N_c of noise control devices that are designed to exhibit high *criterion of viability* and *criterion of promise.* [Eqs. (31)-(36)].

One may now address the speculation that the mean-values of the undulations and the values of the undulation-free *measures* of a set of sprung masses are substantially equal

and are, therefore, independent of the loss factors. The loss factors of the individual sprung masses are here determined by the distributions of the resonance frequencies and the overlap factor (b). [cf. Eqs. (9) and (10).] This statement of independence is found to be only obliquely valid. The validity of this statement holds without qualification only if the number $(N-1)$ of sprung masses in the set approaches infinity so that

$$g(N)f(b) \;<<\; 10^{-1} \quad ; \quad N >> 3 \quad , \tag{A12a}$$

where $g(N)$ and $f(b)$ are stated in Eq. (A10). The statement is only partially valid, to within 10% if

$$g(N)f(b) \lesssim 10^{-1} \quad ; \quad N \geq 3 \quad . \tag{A12b}$$

[cf. Eq. (A11).] When the condition stated in Eq. (A12b) is violated, erosion, in the mean-values, when relevant, and in the values of the measures, progressively sets in. The erosion sets in when

$$g(N)f(b) \gtrsim 10^{-1} \quad ; \quad N \geq 3 \quad , \tag{A12c}$$

and is the more severe the more the inequality stated in Eq. (A12c) is. Appreciable erosion weakens both the *criterion of viability* and the *criterion of promise* and this is the reason that designers deem the overly damped sprung masses; e.g., when $(b) = (8)$, to be detrimental to the performance of the device incorporating them. On the other hand, the detrimental influence of the undulations on the performance of the device is obvious. Therefore, an overlap factor (b) of $(3/2)$ is a design goal that will ensure against undulations on the one hand, and erosion on the other.

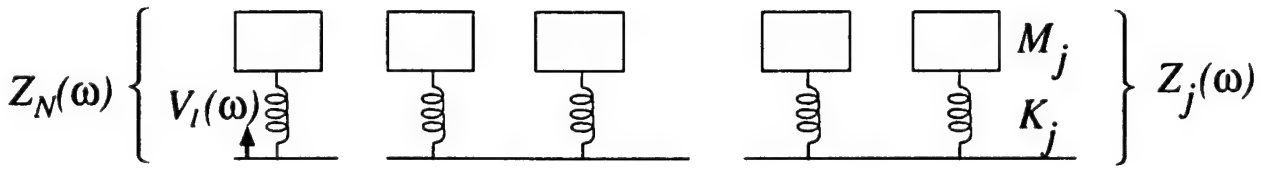

Fig. 1. A sketch of a set of sprung masses acting at a point.

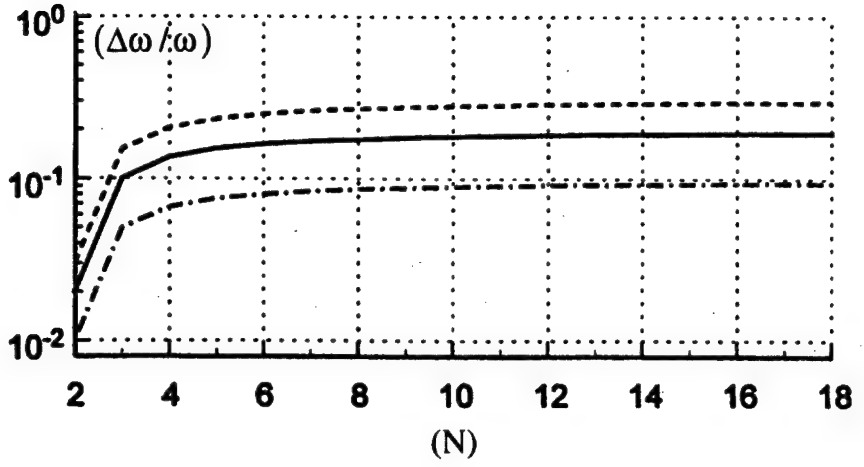

Fig. 2a. The frequency bandwidth $(\Delta\omega/\omega)$ as a function of (N); $2 \le N \le 18$. [cf. Eq. (13a).] — · — · — $\gamma = 0.2$, $\eta = 0.01$; ——— $\gamma = 0.4$, $\eta = 0.02$; $\gamma = 0.6$, - - - - - $\eta = 0.03$.

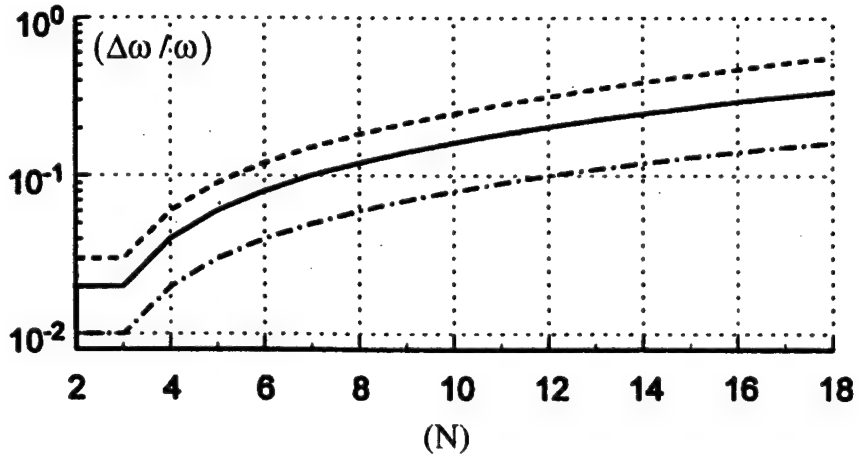

Fig. 2b. The frequency bandwidth $(\Delta\omega/\omega)$ as a function of (N); $2 \le N \le 18$. [cf. Eq. (13b).] — · — · — $\gamma_o = \eta = 0.01$; ——— $\gamma_o = \eta = 0.02$; - - - - - $\gamma_o = \eta = 0.03$.

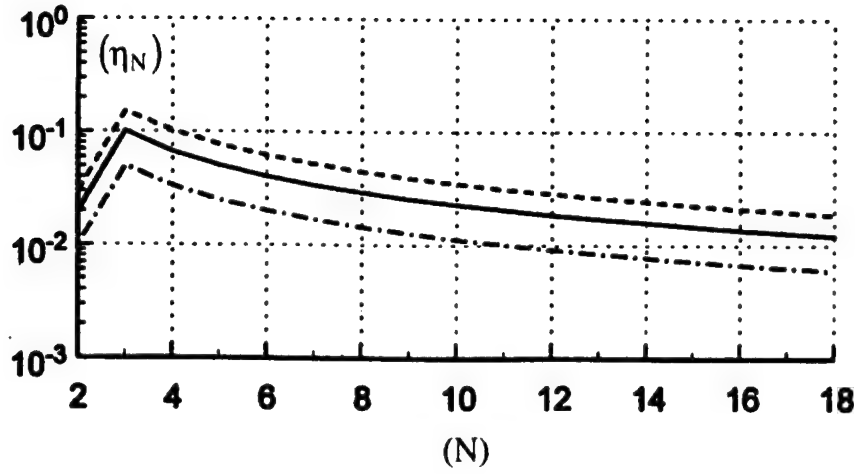

Fig. 3a. The *on the average* loss factor η_N as a function of (N); $2 \leq N \leq 18$. [cf. Eqs. (9a) and (13a).] — · — · — $\gamma = 0.2$, $\eta = 0.01$; ——— $\gamma = 0.4$, $\eta = 0.02$; - - - - - $\gamma = 0.6$, $\eta = 0.03$.

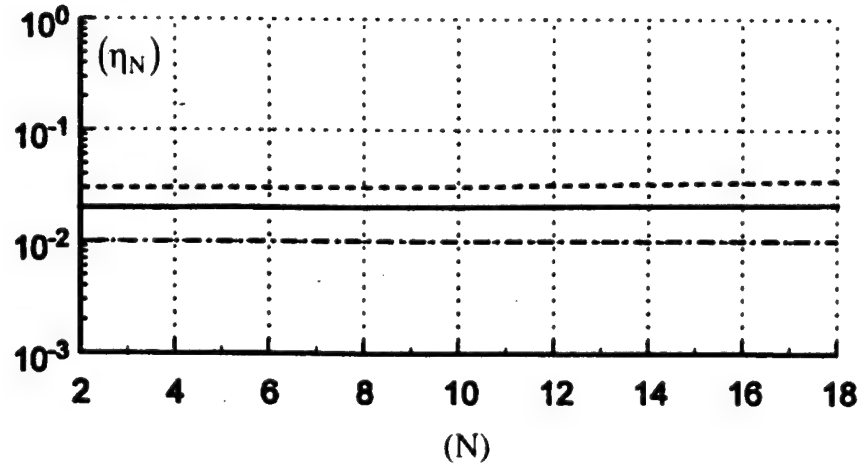

Fig. 3b. The *on the average* loss factor η_N as a function of (N); $2 \leq N \leq 18$. [cf. Eqs. (9a) and (13b).] — · — · — $\gamma_o = \eta = 0.01$; ——— $\gamma_o = \eta = 0.02$; - - - - - $\gamma_o = \eta = 0.03$.

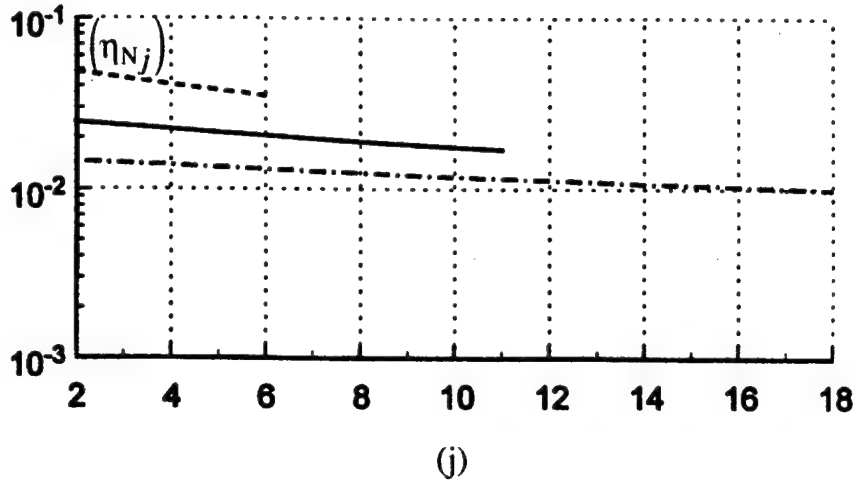

a. $\gamma = 0.4$; $\eta = 0.02$. [cf. Eq. (13a).]

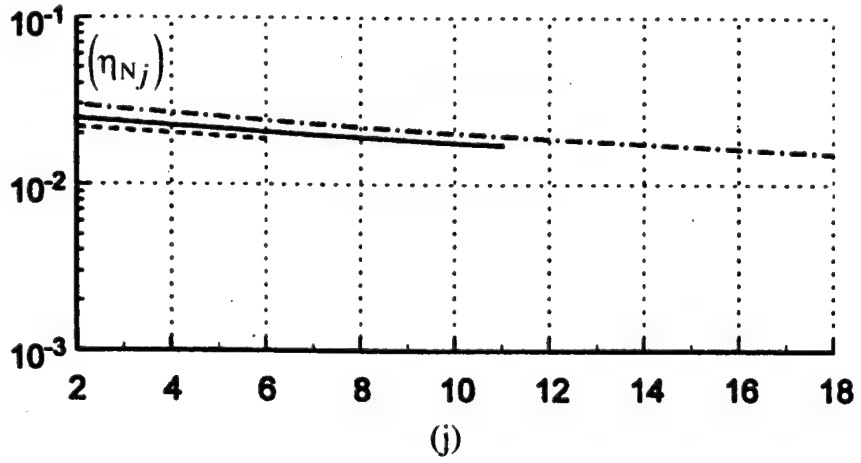

b. $\gamma_o = \eta = 0.02$. [cf. Eq. (13b).]

Fig. 4. The *local* loss factor (η_{Nj}) as a function of (j). [cf. Eq. (9b).] The overlap factor (b) is equal to (3/2). [cf. Eq. (10).] – – – – – $N = 6$; ——— $N = 11$; — · — · — $N = 18$.

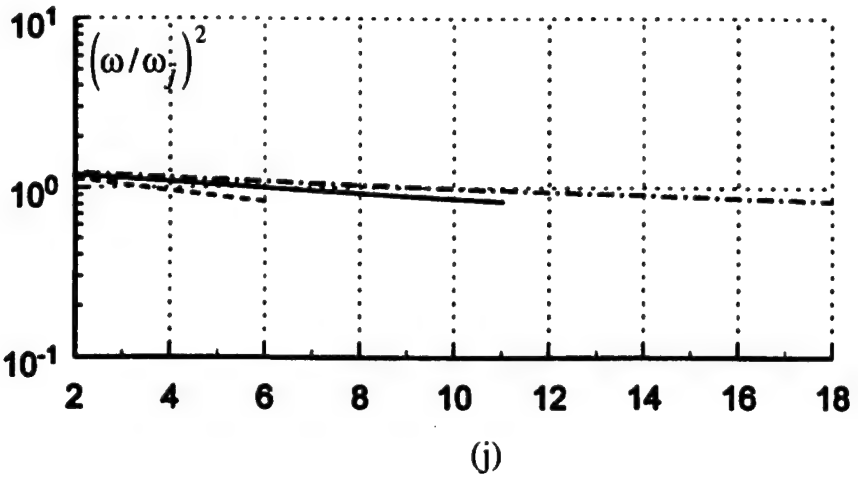

a. $\gamma = 0.4$. [cf. Eq. (13a).]

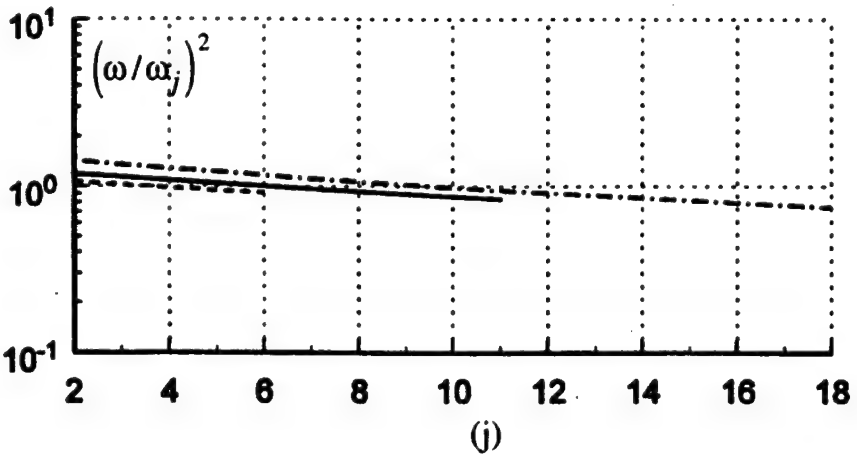

b. $\gamma_o = 0.02$. [cf. Eq. (13b).]

Fig. 5. The normalized quadratic resonance frequency $(\omega/\omega_1)^2$, as a function of (j). [cf. Eq. (12).] - - - - - $N = 6$; ——— $N = 11$; — · — · —; $N = 18$.

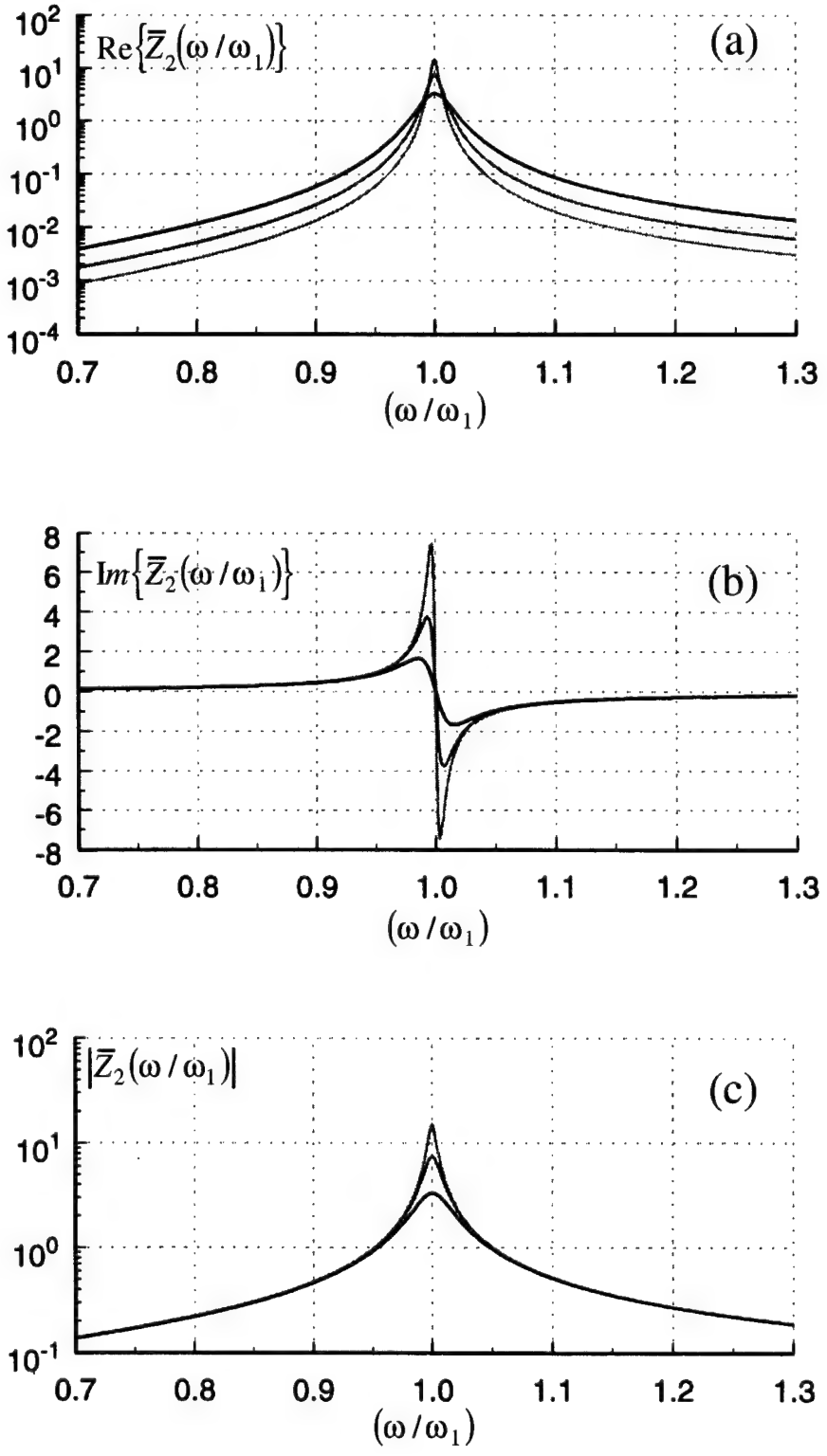

Fig. 6. The normalized quantities relating to the normalized joint impedance $\bar{Z}_N(\omega)$, of a set of $(N-1)$ sprung masses as functions of (ω/ω_1). The set is defined by $N=2$, $a=10$ and $\eta = 2x10^{-2}$. Light curves $\eta_2 = 6.7x10^{-3}$, darker curves $\eta_2 = 1.33x10^{-2}$ and darkest curves $\eta_2 = 3x10^{-2}$.

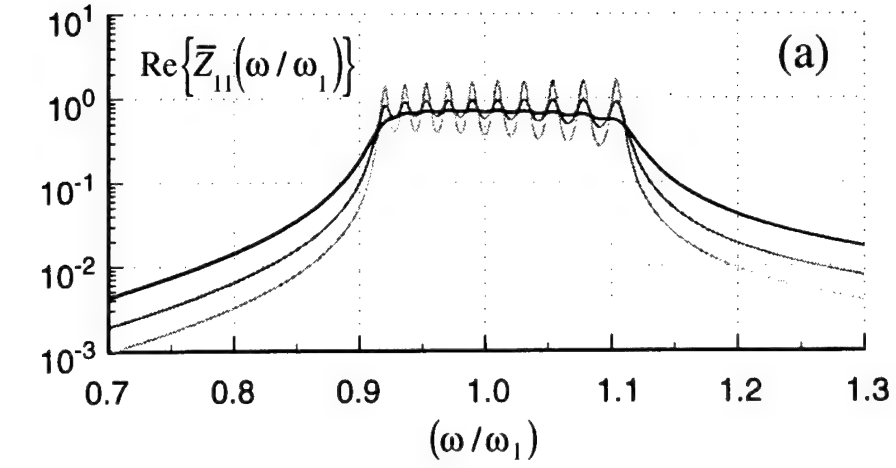

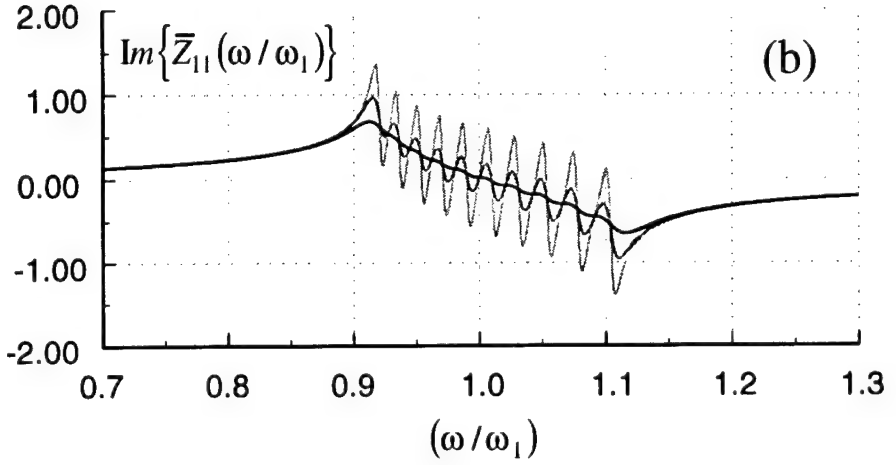

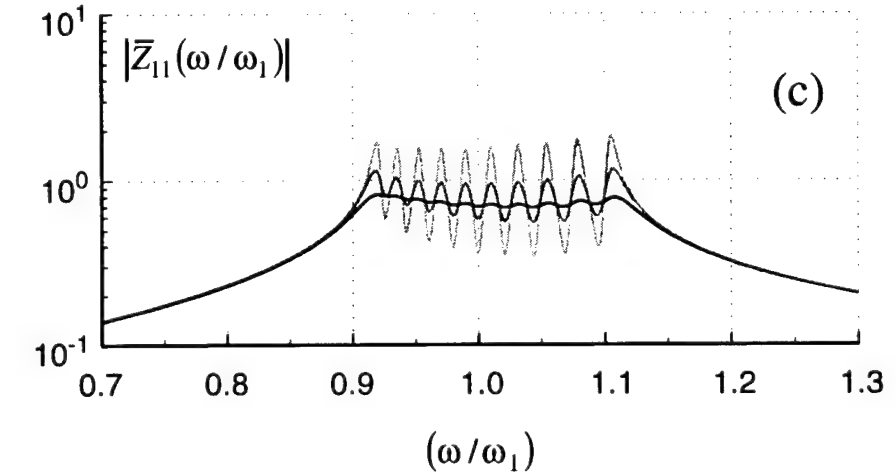

Figs. 7. Normalized joint impedance $\bar{Z}_N(\omega/\omega_1)$ as a function of (ω/ω_1) of a set of $(N-1)=10$ sprung masses. [cf. Eq. (20).] The set is defined by $N=11$, by $a=10$, by $\gamma_o=\eta=0.02$ and by $\gamma=0.4$. [cf. Eq. (13a).] Light curves $b=(1/3)$, darker curves $b=(2/3)$ and darkest curves $b=(3/2)$. [cf. Eq. (10).] Employs *on the average* loss factors. [cf. Eq. (9a).]

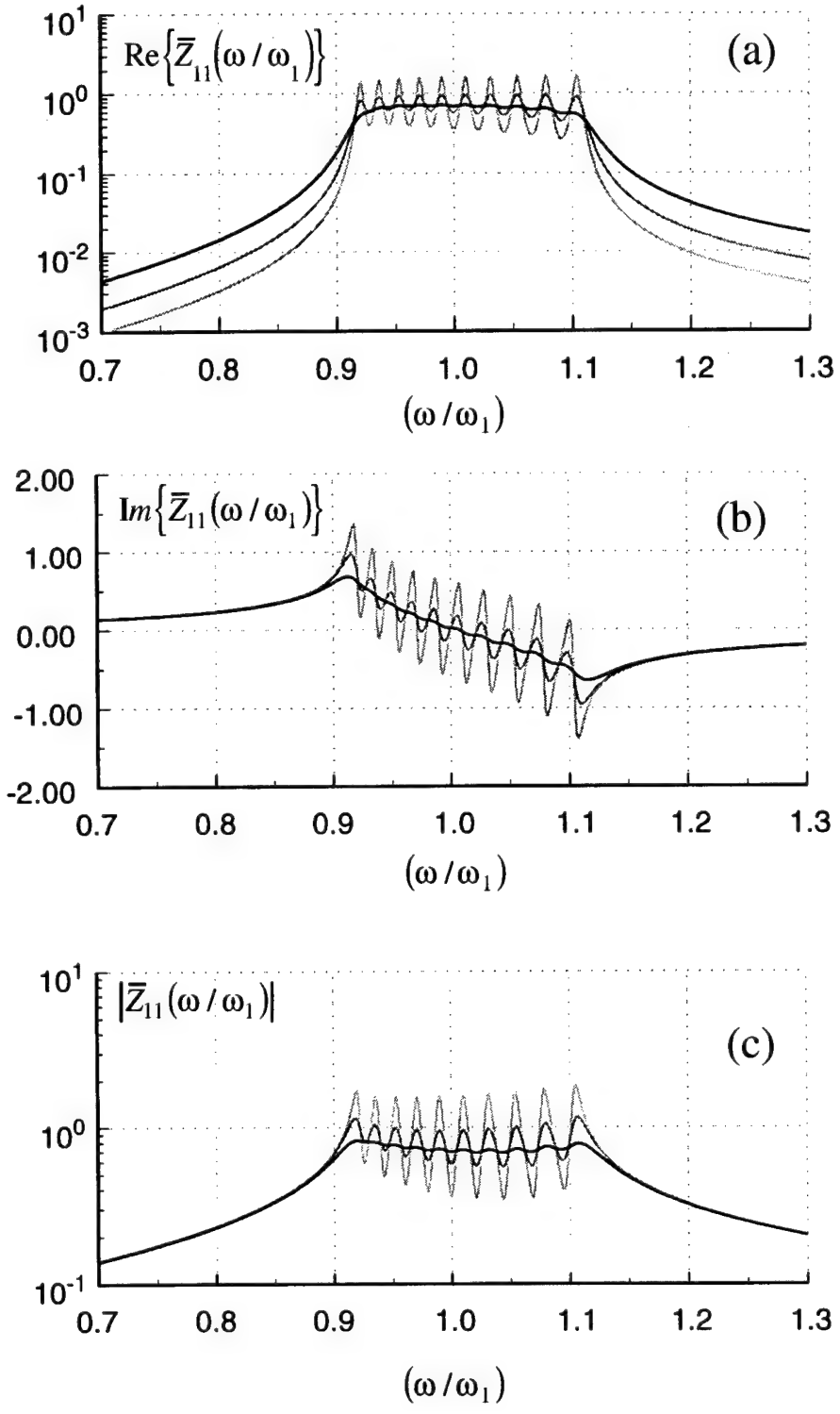

Fig. 8. Repeats Fig. 7 except that *local* loss factors are employed. [cf. Eq. (9b).]

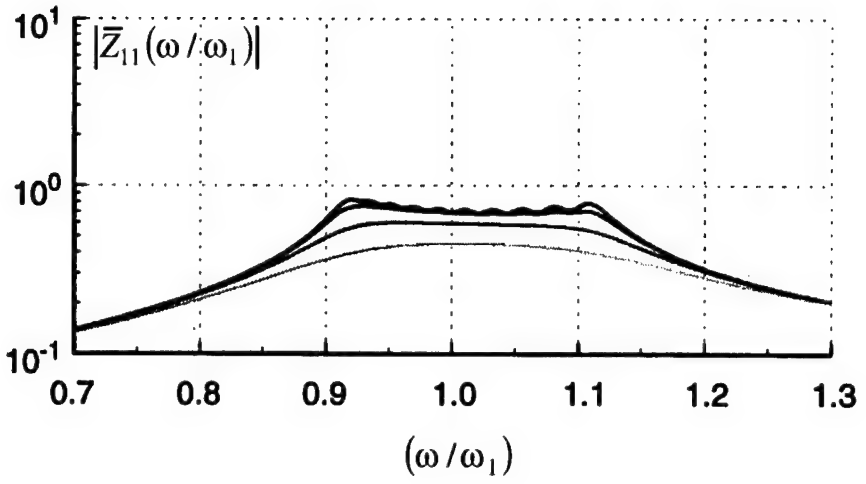

Fig. 9. Repeats Fig. 8c except that the values of the overlap factor (b) are: $(3/2)$ (darkest curve) 2, 4, and 8 (lightest curve). [cf. Eq. (10).]

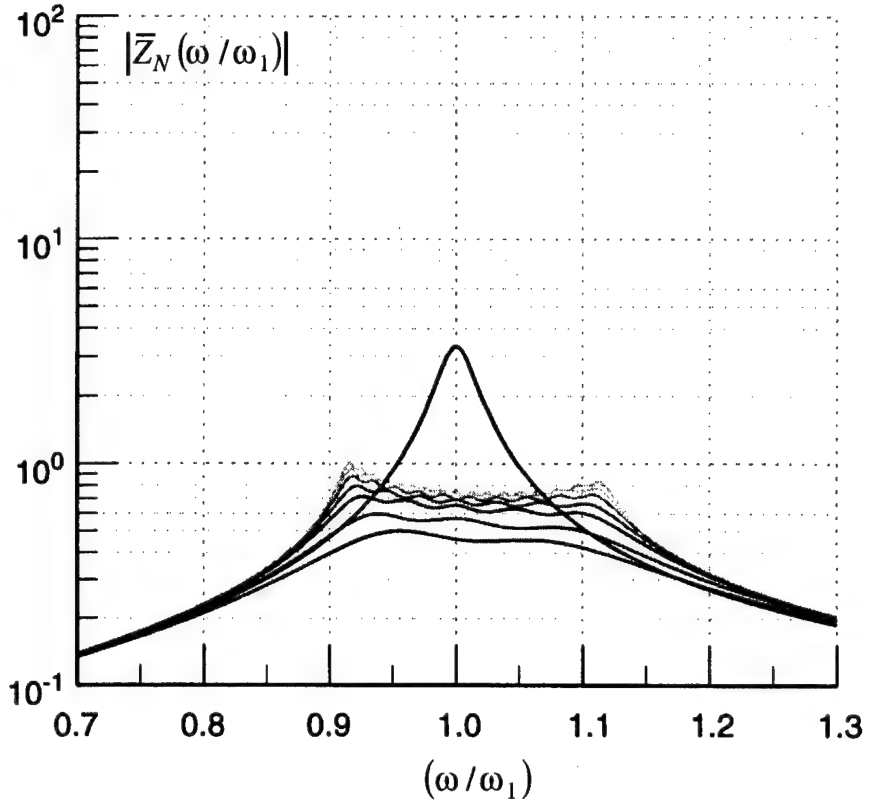

a. $\gamma = 0.4$ and $\eta = 0.02$. [cf. Eq. (13a).]

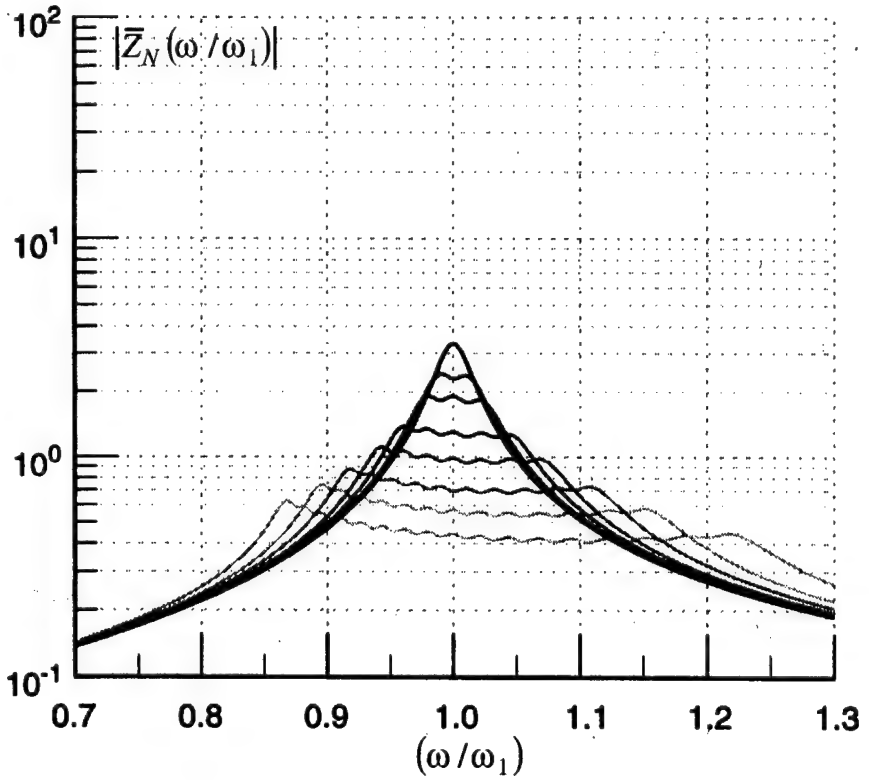

b. $\gamma_o = \eta = 0.02$. [cf. Eq. (13b).]

Fig. 10. The absolute values of the normalized joint impedance $|\bar{Z}_N(\omega/\omega_1)|$ as a function of (ω/ω_1) for $N = 2$ (darkest curve), 3, 4, 6, 8, 11, 14 and 18 (lightest curve) with the overlap factor $b = (3/2)$. [cf. Eq. (10).]

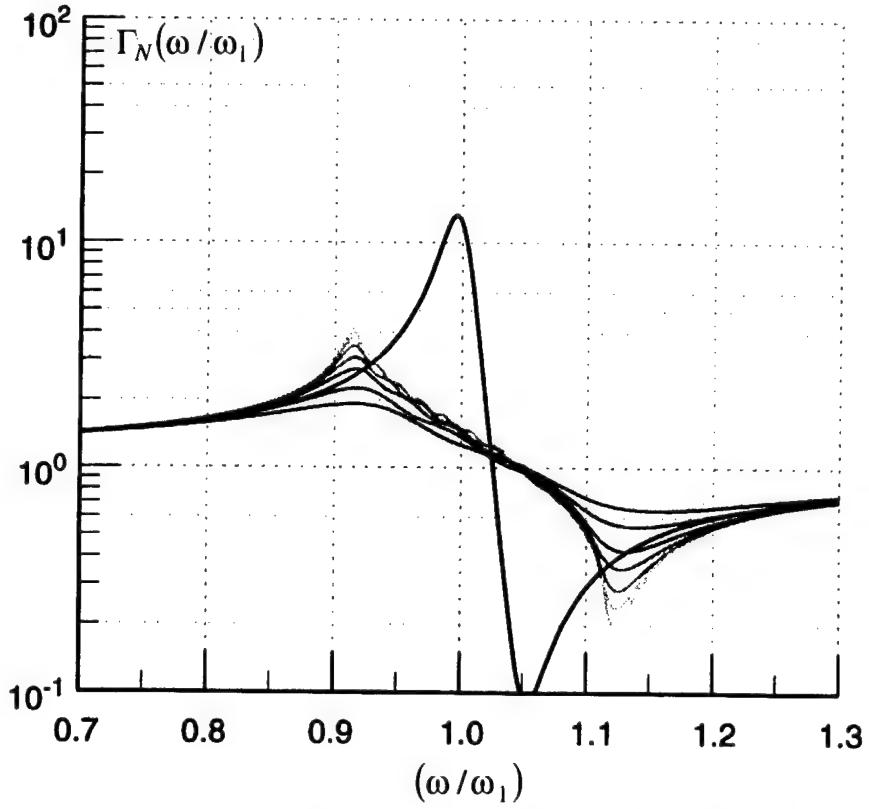

a. Computed $\Gamma_{1N}(\omega/\omega_1)$ from Fig. 10a and $\overline{Z}_1(\omega/\omega_1) = i(\omega/\omega_1)$. [cf. Eq. (23a).]

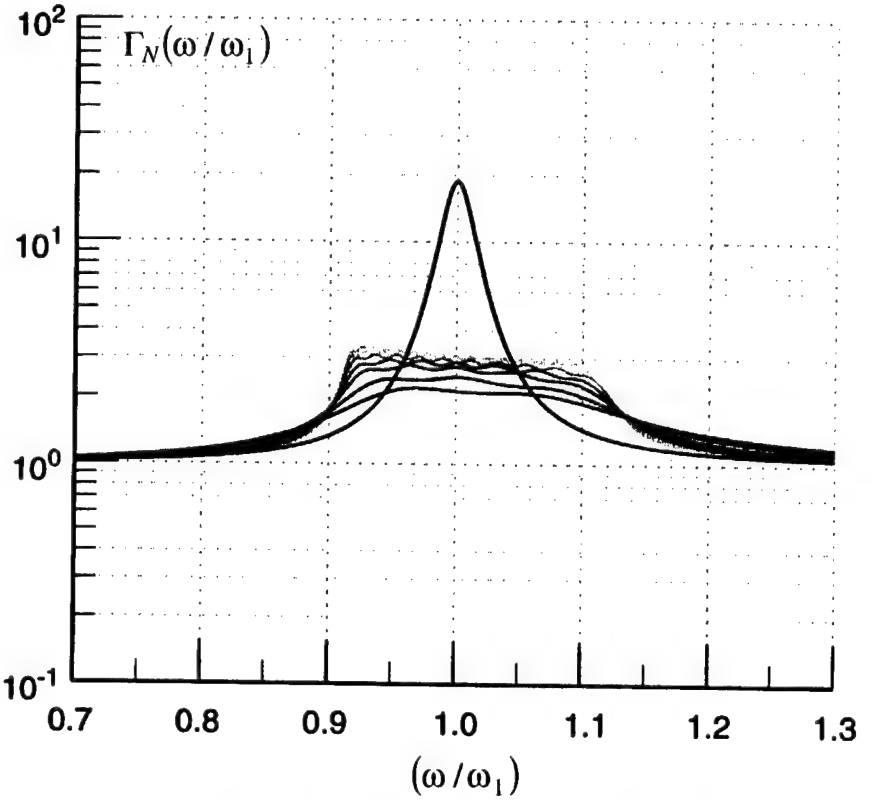

b. Computed $\Gamma_{1N}(\omega/\omega_1)$ from Fig. 10a and $\overline{Z}_1(\omega/\omega_1) = 1$ [cf. Eq. (23b).]

Fig. 11. The overall gain $\Gamma_{1N}(\omega/\omega_1)$ and the normalized overall gain $\overline{\Gamma}_{1N}(\omega/\omega_1)$ as functions of (ω/ω_1). [cf. Eq. (22).]

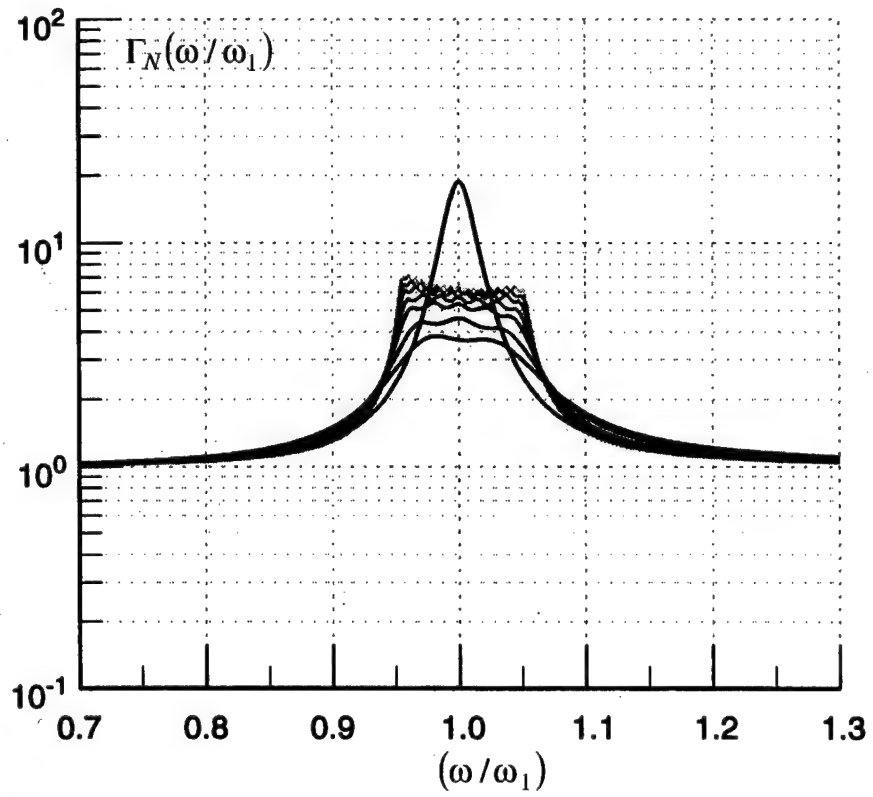

c. Repeats Fig. 11b except that (γ) is halved, from 0.4 to 0.2. The value of $N_o = 6$. [cf. Eq. (13c).]

Fig. 11. (Cont.)

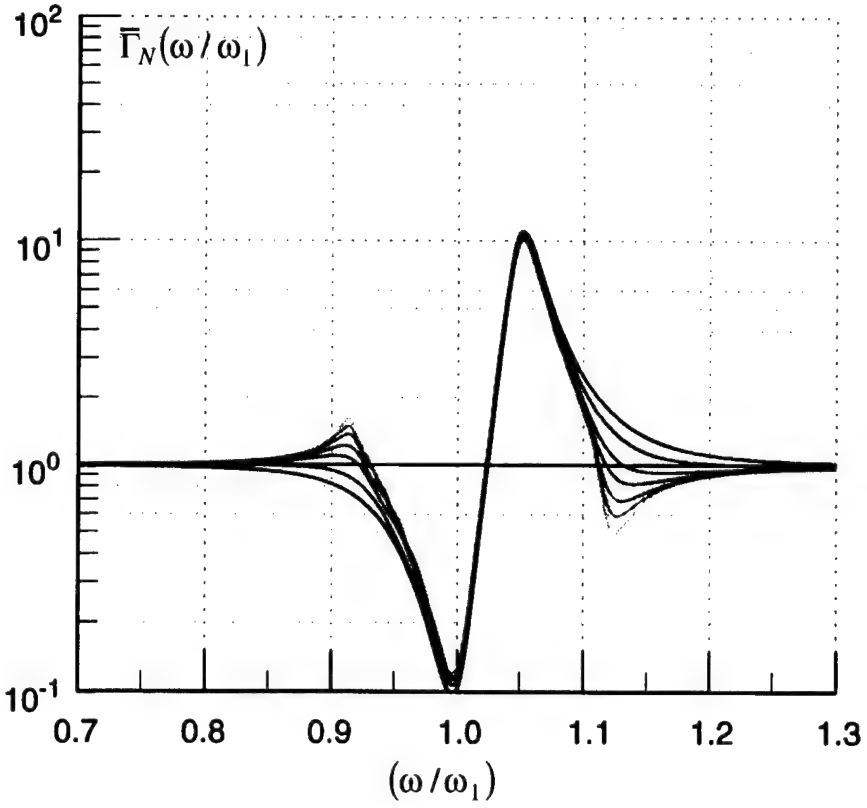

d. Computed $\bar{\Gamma}_{1N}(\omega/\omega_1)$ from Fig. 10a and $\bar{Z}_1(\omega/\omega_1) = i(\omega/\omega_1)$. [cf. Eq. (23a).]

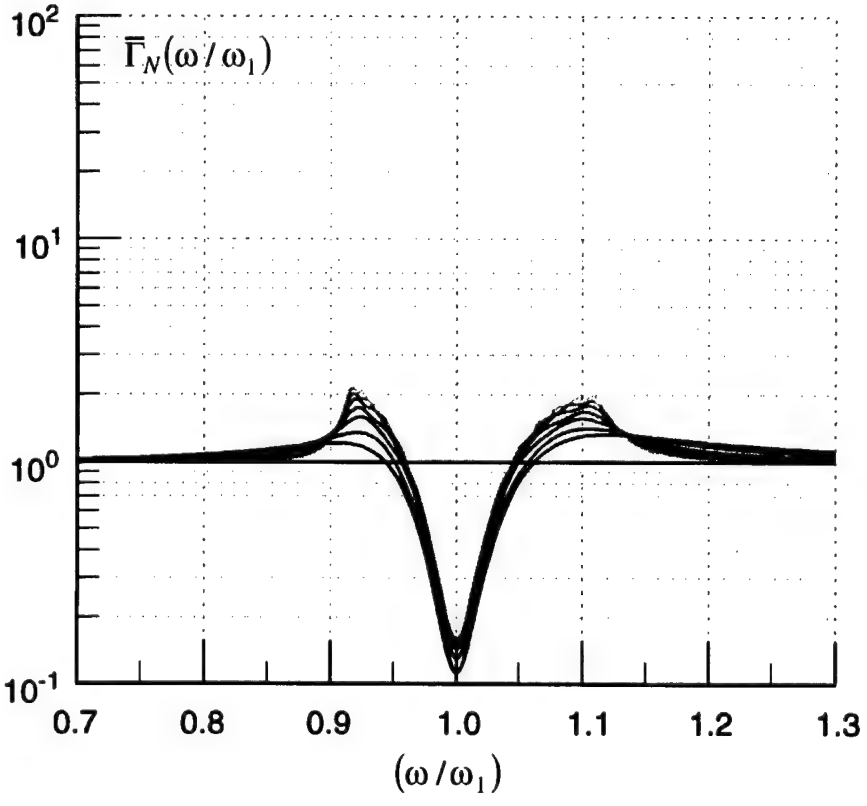

e. Computed $\bar{\Gamma}_{1N}(\omega/\omega_1)$ from Fig. 10a and $\bar{Z}_1(\omega/\omega_1) = 1$. [cf. Eq. (23a).]

Fig. 11. (Cont.)

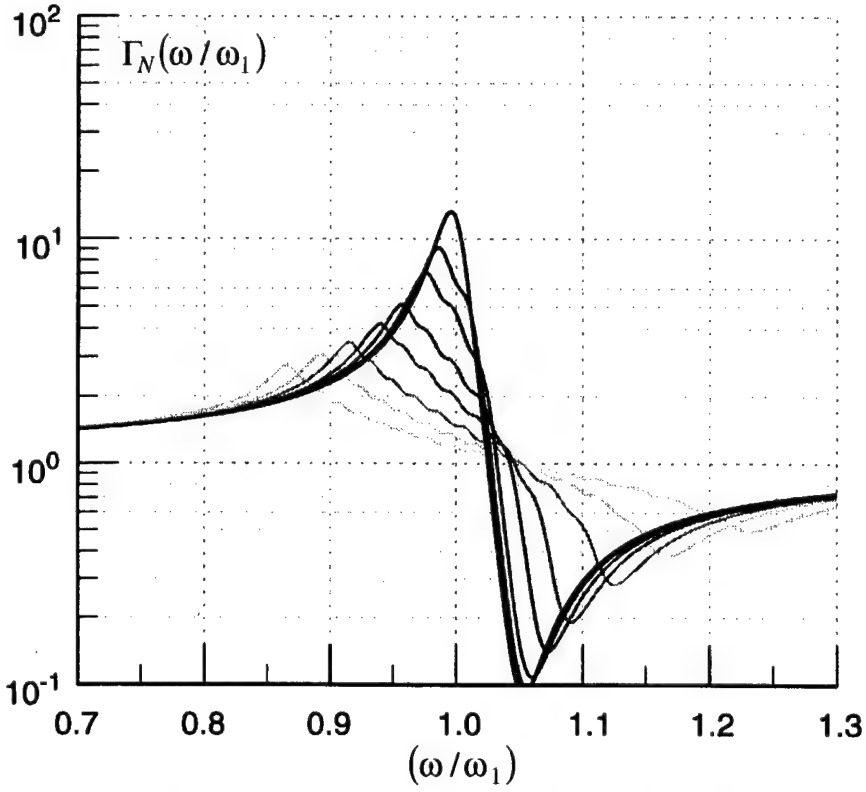

a. Computed $\Gamma_{1N}(\omega/\omega_1)$ from Fig. 10b and $\overline{Z}_1(\omega/\omega_1) = i(\omega/\omega_1)$. [cf. Eq. (23a).]

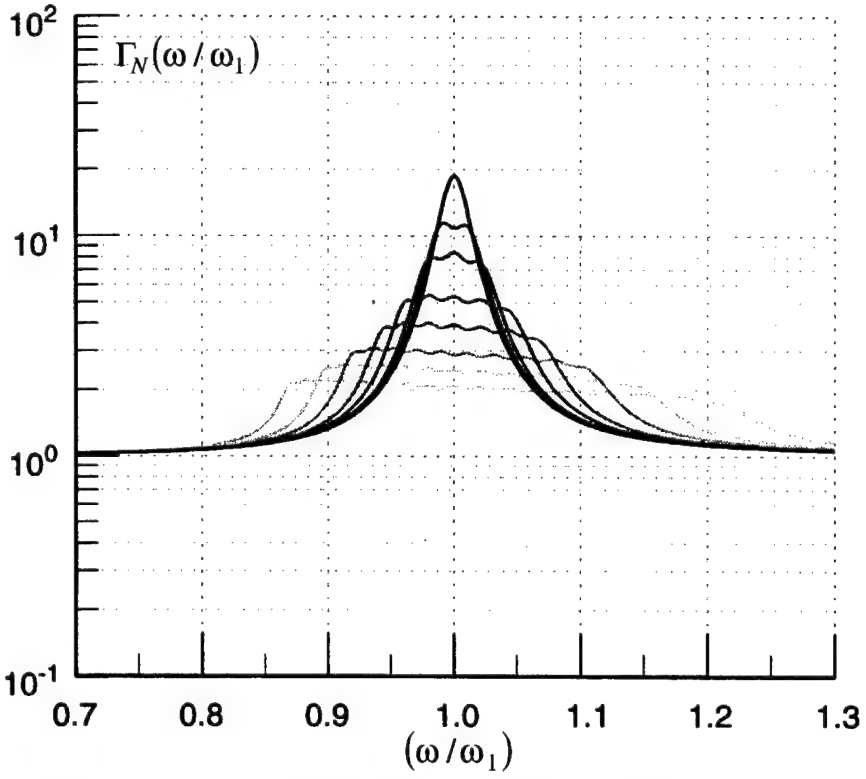

b. Computed $\Gamma_{1N}(\omega/\omega_1)$ from Fig. 10b and $\overline{Z}_1(\omega/\omega_1) = 1$. [cf. Eq. (23b).]

Fig. 12. The overall gain $\Gamma_{1N}(\omega/\omega_1)$ and the normalized overall gain $\overline{\Gamma}_{1N}(\omega/\omega_1)$ as functions of (ω/ω_1). [cf. Eq. (22).]

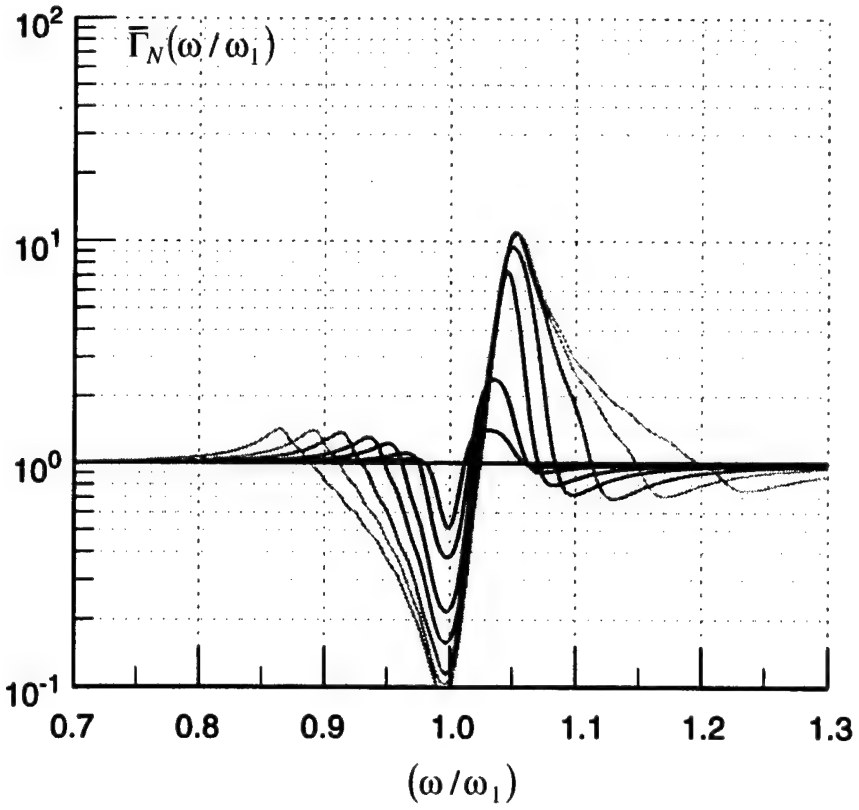

c. Computed $\bar{\Gamma}_{1N}(\omega/\omega_1)$ from Fig. 10b and $\bar{Z}_1(\omega/\omega_1) = i(\omega/\omega_1)$. [cf. Eq. (23a).]

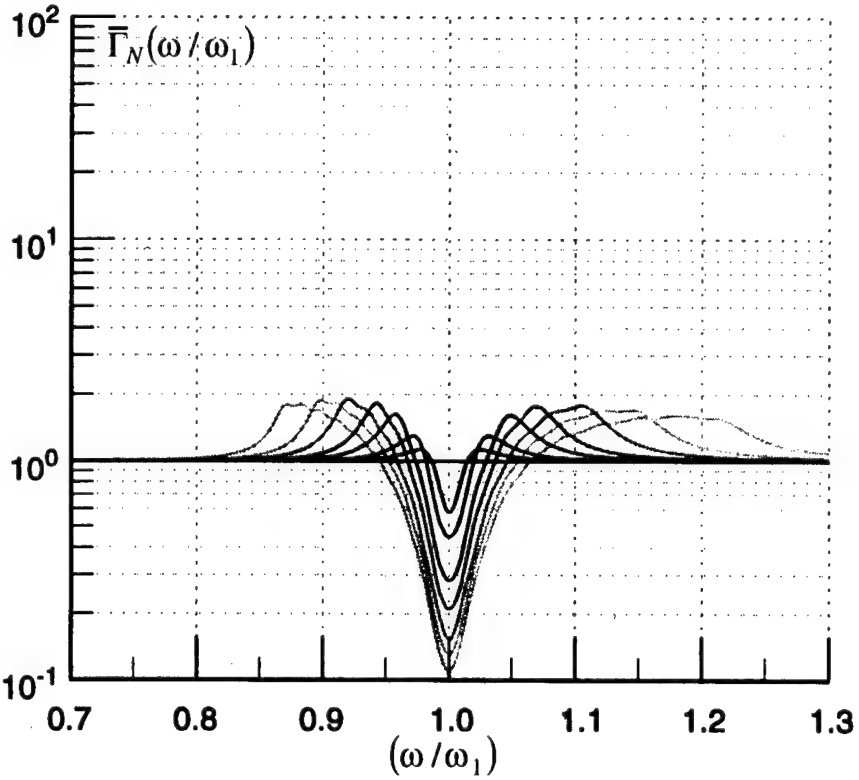

d. Computed $\bar{\Gamma}_{1N}(\omega/\omega_1)$ from Fig. 10b and $\bar{Z}_1(\omega/\omega_1) = 1$. [(cf. Eq. (23b).]

Fig. 12. (Cont.)

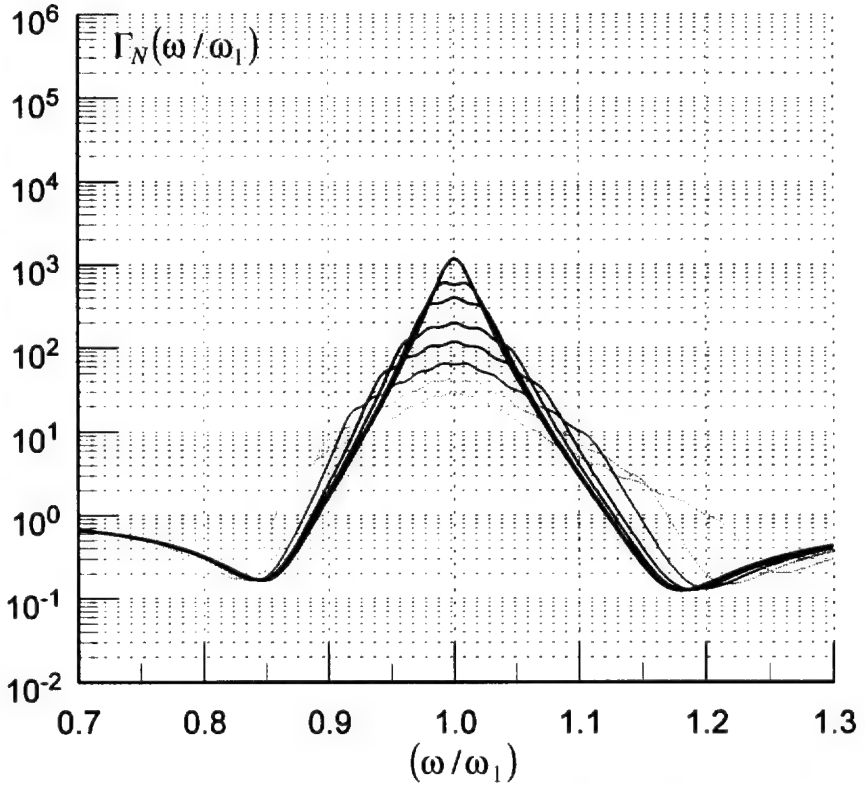

a. Computed $\Gamma_{1N}(\omega/\omega_1)$ from Fig. 10b and $\overline{Z}_1(\omega/\omega_1)$ as specified in Eq. (23a) and with $\eta_1 = 10^{-1}$.

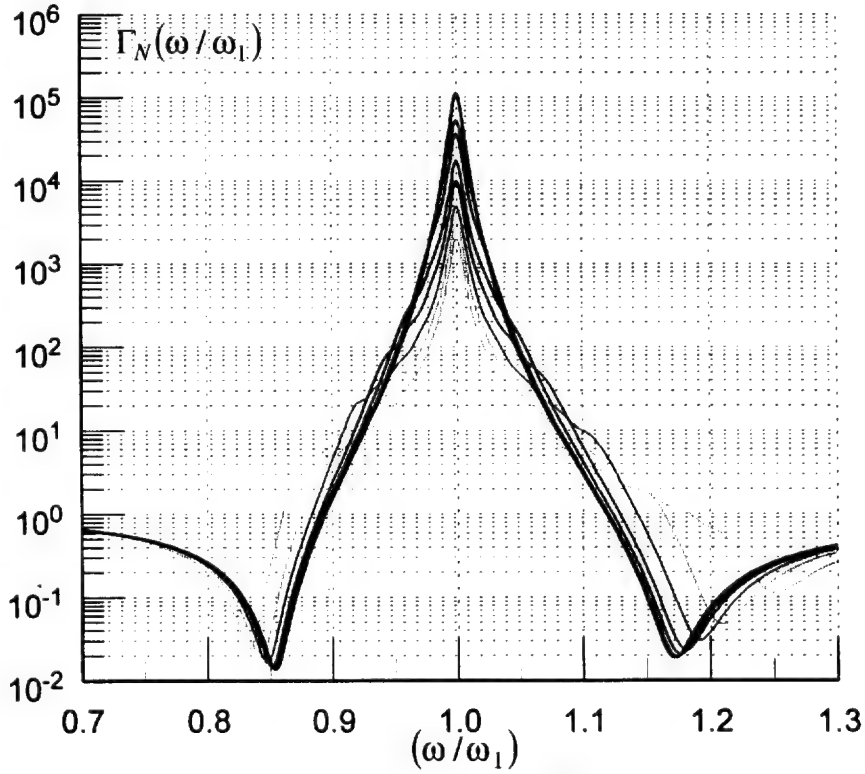

b. Computed $\Gamma_{1N}(\omega/\omega_1)$ from Fig. 10b and $\overline{Z}_1(\omega/\omega_1)$ as specified in Eq. (23c) and with $\eta_1 = 10^{-2}$.

Fig. 13. The overall gain $\Gamma_{1N}(\omega/\omega_1)$ and the normalized overall gain $\overline{\Gamma}_{1N}(\omega/\omega_1)$ as functions of (ω/ω_1). [cf. Eq. (22) and note change of ordinate scales from those in Figs. 11 and 12.]

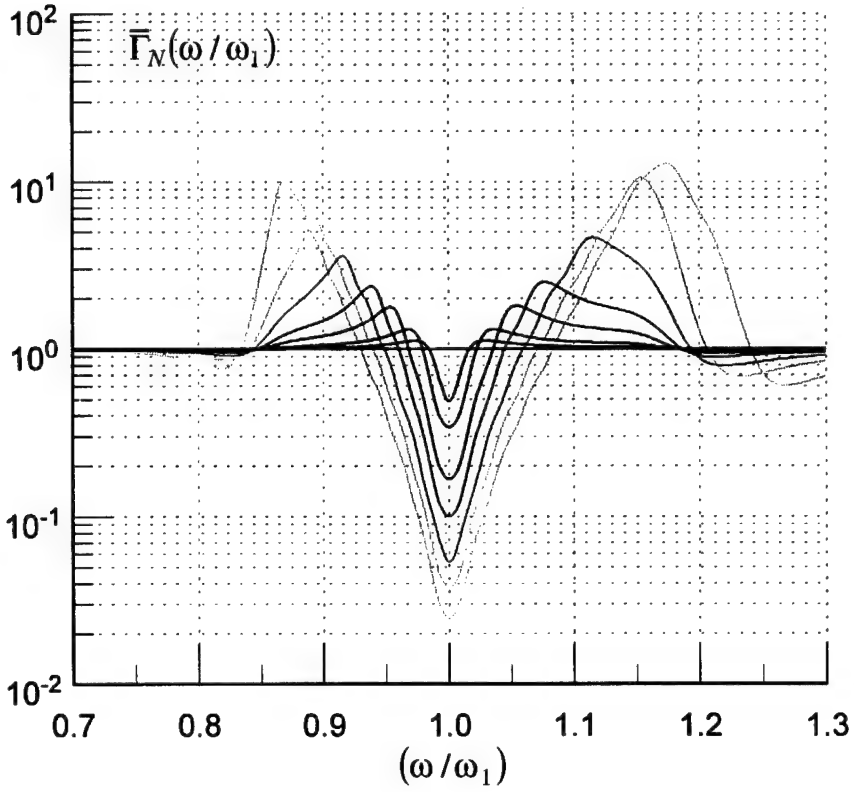

c. Computed $\bar{\Gamma}_{1N}(\omega/\omega_1)$ from Fig. 10b and $\bar{Z}_1(\omega/\omega_1)$ as specified in Eq. (23c) and with $\eta_1 = 10^{-1}$.

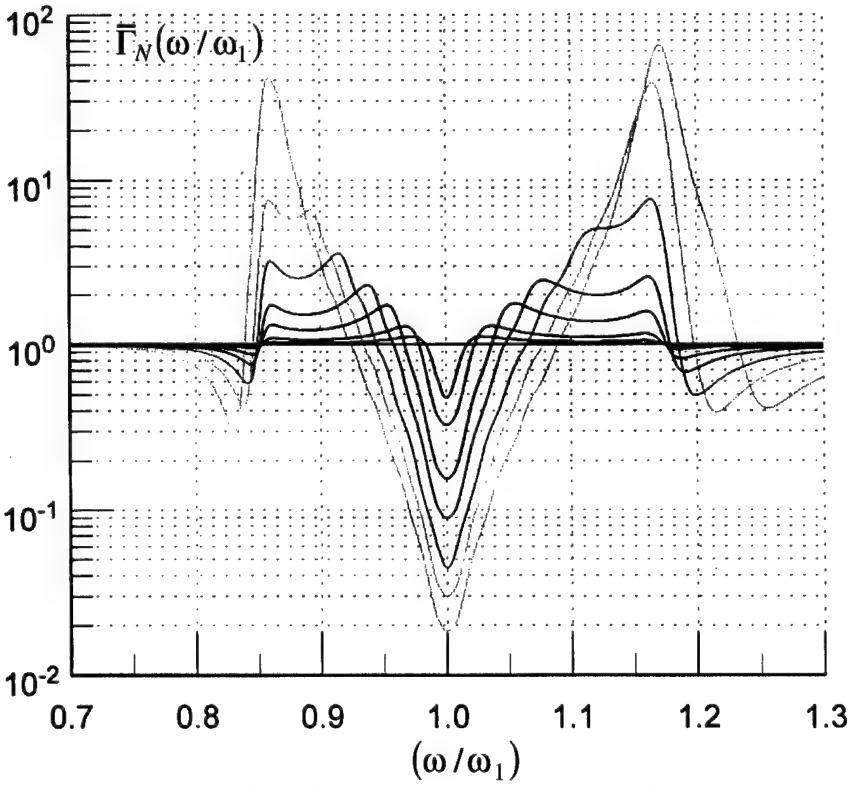

d. Computed $\bar{\Gamma}_{1N}(\omega/\omega_1)$ from Fig. 10b and $\bar{Z}_1(\omega/\omega_1)$ as specified in Eq. (23c) and with $\eta_1 = 10^{-2}$.

Fig. 13. (Cont.)

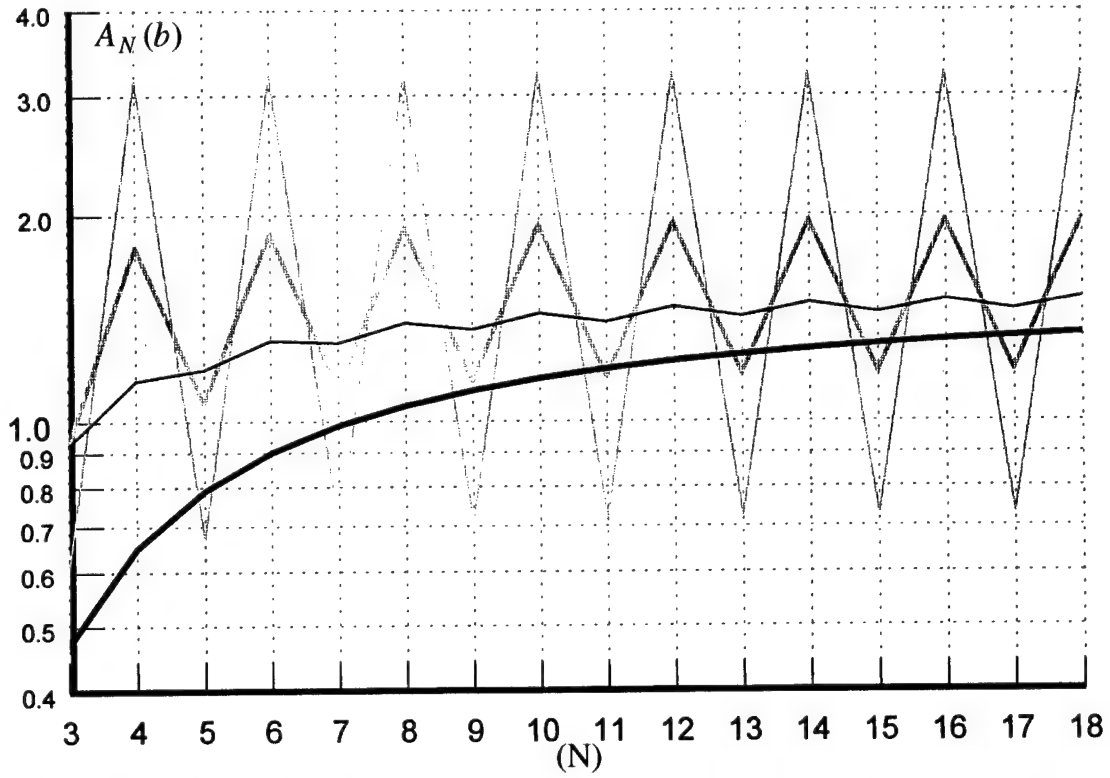

Fig. 14a. The *measure* $A_N(b)$ as a function of (N). [cf. Eq. (30a).] The values of the overlap factors (b) are: $(1/3)$ (lightest curve), $(2/3)$, $(3/2)$ and (4) (darkest curve).

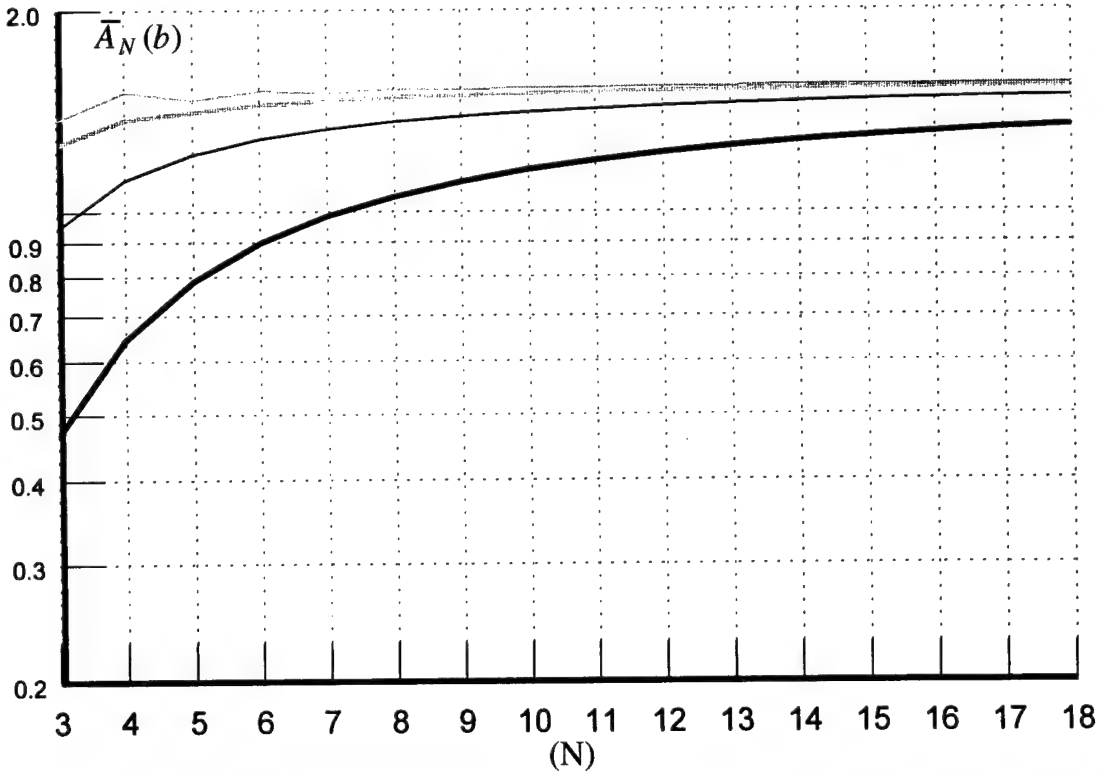

Fig. 14b. The undulations-free *measure* $\bar{A}_N(b)$ as a function of (N). [cf. Eq. (30b).] the values of the overlap factor (b) are: $(1/3)$ (lightest curve), $(2/3)$, $(3/2)$ and (4) (darkest curve).

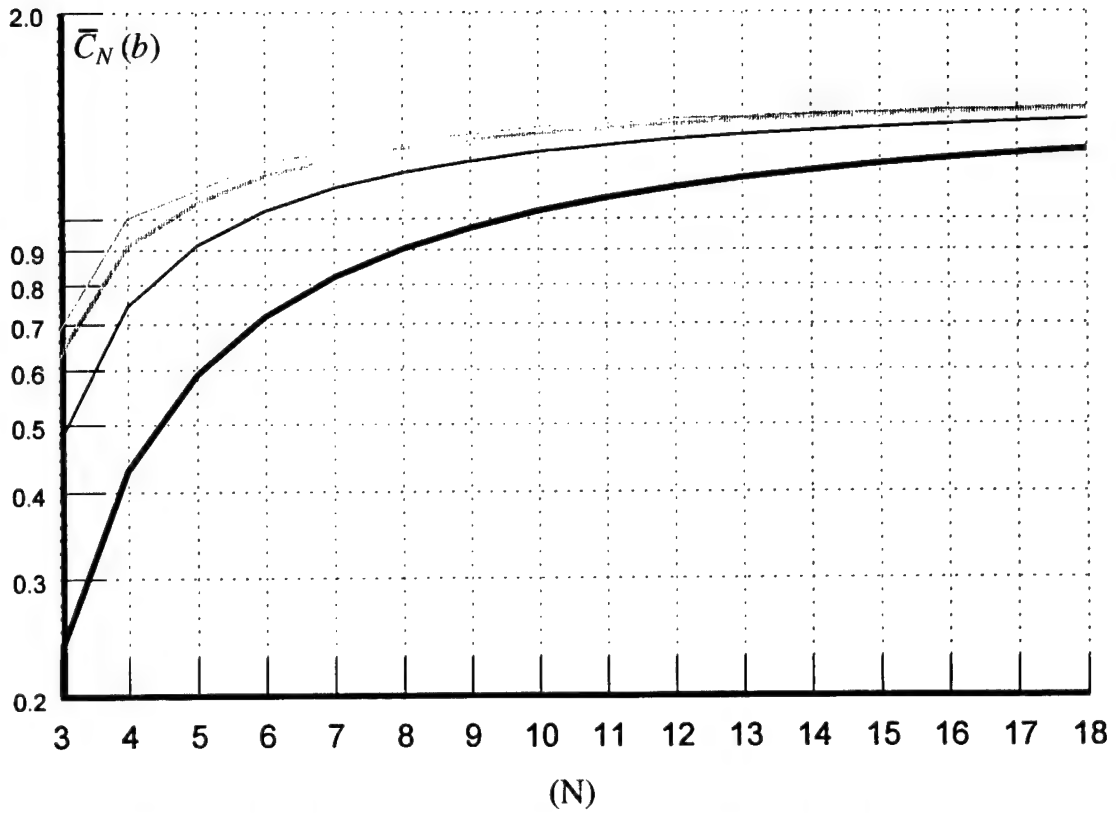

Fig. 14c. The *criterion of promise* $\overline{C}_N(b)$ as a function of (N). [cf. Eqs. (31) and (32).] The values of the overlap factor (b) are: $(1/3)$ (darkest curve), $(2/3)$, $(3/2)$ and (4) (lightest curve).

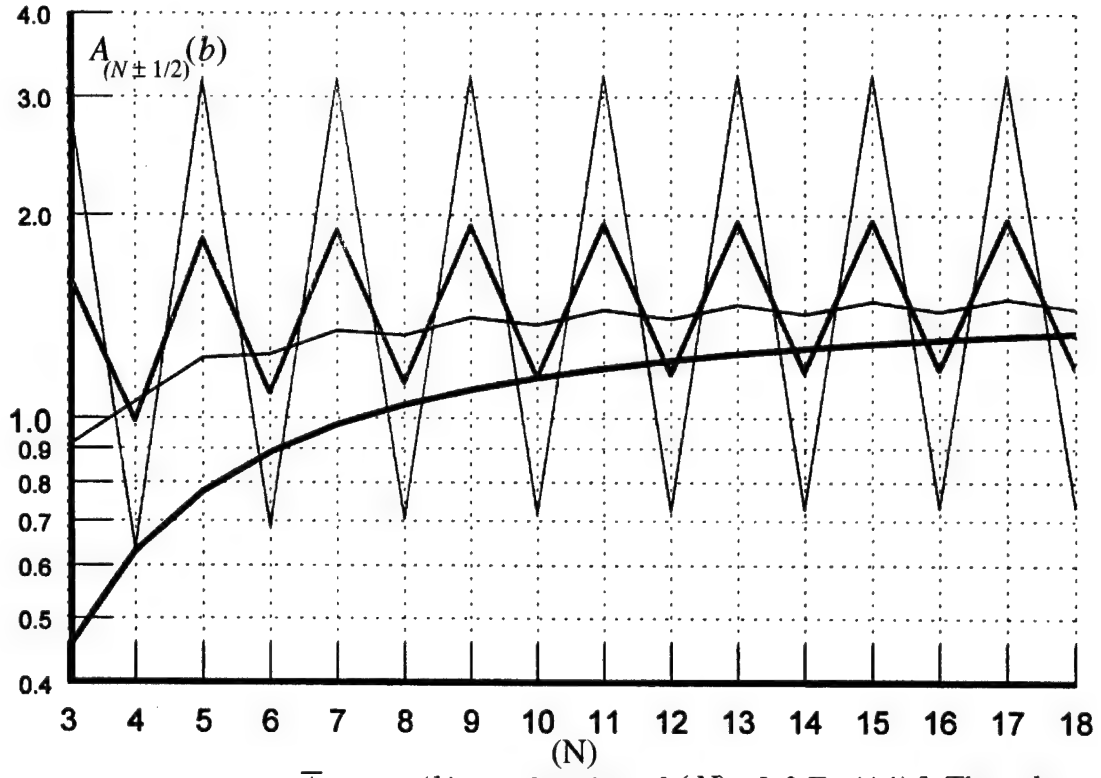

Fig. A1. The *measure* $\overline{A}_{(N\pm 1/2)}(b)$ as a function of (N). [cf. Eq (A1).] The values of the overlap factor (b) are: $(1/3)$ (lightest curve), $(2/3)$, $(3/2)$ and (4) (darkest curve).

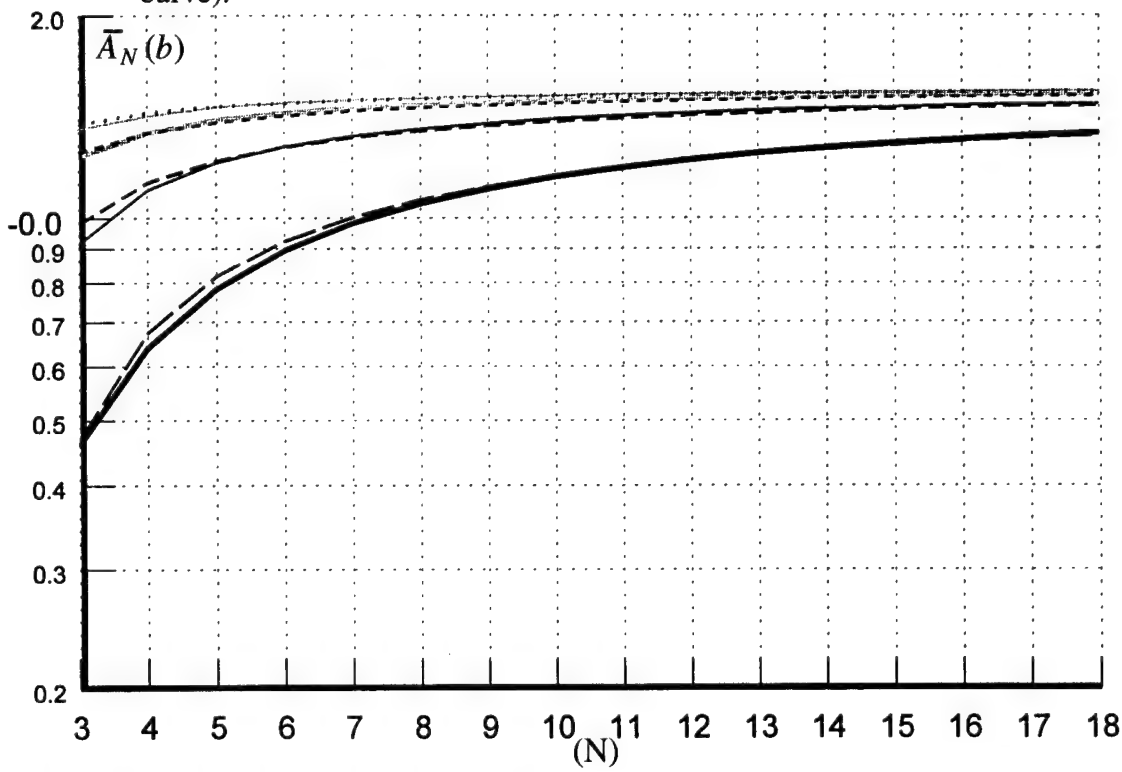

Fig. A2. The undulations-free *measure* $\overline{A}_N(b)$ as a function of (N). [cf. Eq (A3).] The values of the overlap factor (b) are: $(1/3)$ (lightest curve), $(2/3)$, $(3/2)$ and (4) (darkest curve). Superposed is $\overline{A}_N(b)$ as stated in Eqs. (A9) and (A10). These superposed values of $\overline{A}_N(b)$ are depicted by dashed lines.

REFERENCES

1. C. Soize, "Probabilistic structural modeling in linear dynamic analysis of complex mechanical systems," Rech. Aerosp, 1986-3, 23-48 (1986); "A model and numerical method in the medium frequency range for vibroacoustic predictions using the theory of structural fuzzy," J. Acoust. Soc. Am. 94, 849-865 (1993); R. Ohayon and C. Soize, Structural Acoustics and Vibrations (Academic Press, San Diego, 1998).
2. A.D. Pierce, V.W. Sparrow and D.A. Russell, "Fundamental structural acoustics idealizations for structures with fuzzy internals," ASME J. Vib. Acoust. 117, 1-10 (1995).
3. M. Strasberg and D. Feit, "Vibration damping of large structures induced by attached small resonant substructures," J. Acoust. Soc. Am. 99, 335-344 (1996).
4. M. Strasberg, "Continuous structures as 'fuzzy' substructures," J. Acoust. Soc. Am. 100, 3456-3459 (1996).
5. M.J. Brennan, "Wideband vibration neutralizer," Noise Control Eng. J. 45, 201-207 (1997).
6. G. Maidanik, "Power dissipation in a sprung mass attached to a master structure," J. Acoust. Soc. Am. 98, 3527-3533 (1995).
7. K.U. Ingard, Fundamentals of Waves and Oscillations (Cambridge University Press, Cambridge 1988).
8. G. Maidanik and K.J. Becker, "Various loss factors of a master harmonic oscillator that is coupled to a number of satellite harmonic oscillator," Accepted for publication in JASA.
9. M. Strasberg, "Is the dissipation induced by "fuzzy" substructures real or apparent," J. Acoust. Soc. Am. 102, 3130 (1997).

10. G. Maidanik and K.J. Becker, "Various loss factors of a master harmonic oscillator that is coupled to a number of satellite harmonic oscillator," Submitted for publication in JASA.

11. R.H. Lyon, Statistical Energy Analysis of Dynamic Systems: Theory and Applications (MIT, Cambridge, 1975); R.H. Lyon and R.G. DeJong, Theory and Application of Statistical Energy Analysis (Butterworth-Heinemann, Boston, 1995).

12. E. Skudrzyk, "The mean-value method of predicting the dynamic response of complex vibrators," J. Acoust. Soc. Am. 67, 1105-1135 (1980).

13. G. Maidanik and K.J. Becker, "Noise control of a master harmonic oscillator that is coupled to a set of satellite harmonic oscillator," Submitted for publication .

14. I.S. Gradshteyn and I.M. Ryzhik, Table of Integrals, Series and Products (Translation edited by A. Jeffrey, p. 35. Academic Press, New York (1965).

INITIAL DISTRIBUTION

Copies

3 NAVSEA 03T2
- 2 Taddeo
- 1 Becker

5 ONR/ONT
- 1 334 Tucker
- 1 334 Radlinski
- 1 334 Vogelsong
- 1 334 Main
- 1 Library

4 NRL
- 1 5130 Bucaro
- 1 5130 Williams
- 1 5130 Photiadis
- 1 Library

4 NUWC/NPT
- 1 Sandman
- 1 Harari
- 1 3332 Lee
- 1 Library

2 DTIC

2 Johns Hopkins University
- 1 Green
- 1 Dickey

1 Applied Physics Lab
Johns Hopkins University
Library

3 ARL/Penn State University
- 1 Burroughs
- 1 Biancardi
- 1 Hwang

1 Cambridge Collaborative
Manning

1 Cambridge Acoustical Associate
Garrelick

1 J. G. Engineering Research
Greenspan

1 MIT
- 1 Dyer

1 Catholic Uni. of Am. Eng.
Dept.
McCoy

Copies

2 Boston University
- 1 Pierce
- 1 Barbone

1 Penn State University
- 1 Koopman

2 Virginia Tech
- 1 Knight
- 1 Fuller

Copies	Code	Name
1	01B	Sevik
1	011	Corrado
2	0112	Douglas Halsall
1	20	
1	2040	Everstine
1	70	Covich
3	7015	Fisher Hamly Vendittis
1	7020	Strasberg
3	7203	Dlubac
6	7250	Shang Maga Vasudevan Carroll Niemiec Bowers
1	726	Szilagyi
1	842	Graesser
2	3421	(TIC-Carderock)

DEPARTMENT OF THE NAVY
NAVAL SURFACE WARFARE CENTER
CARDEROCK DIVISION

CARDEROCK DIVISION HEADQUARTERS
DAVID TAYLOR MODEL BASIN
9500 MACARTHUR BOULEVARD
WEST BETHESDA, MD 20817-5700

IN REPLY REFER TO:

9073
703/98015
1 SEP 98

From: Commander, Carderock Division, Naval Surface Warfare Center (CDNSWC)
To: Commander, Naval Sea Systems Command (NAVSEA 03T2)

Subj: REPORT TRANSMITTAL

Encl: (1) NSWCCD-SIG-C98/149-7030 "Multiple-Sprung Masses for Wideband Noise Control", August 1998

1. Enclosure (1) is forwarded to NAVSEA for your utilization.

2. Questions or comments on this issue should be addressed to Dr. Gideon Maidanik, CDNSWC, Code 703 at 301-227-1292.

P.M. COVICH
By direction

Copy with enclosure to:

NAVSEA	03T2	Taddeo, Becker
ONR/ONT	334	Tucker, Radlinski, Vogelsong, Main, Library
NRL	5130	Bucaro, Williams, Photiadis, Library
NUWC/NPT		Sandman, Harari, Lee, Library
DTIC (2)		
JHU		Green, Dickey
APL/JHU		Library
ARL/PSU		Burroughs, Biancardi, Hwang
Cambridge Collaborative		Manning
CAA		Garrelick
JGE		Greenspan
MIT		Dyer
CUAE		McCoy
Boston Univ.		Pierce, Barbone
PSU		Koopman (2)
Virginia Tech		Knight, Fuller